Diplomarbeit

BRAF V600E Testing in Malignant Melanoma: Analytical Comparison of Immunohistochemistry versus Genotyping

eingereicht von

Anna Mueller

zur Erlangung des akademischen Grades

Doktor(in) der gesamten Heilkunde

(Dr. med. univ.)

an der

Medizinischen Universität Graz

ausgeführt an der

Universitätsklinik für Dermatologie und Venerologie

unter der Anleitung von

Univ.-Prof. Dr.med.univ. Peter Wolf

und

Priv.-Doz.in Dr.in med.univ. Ariane Aigelsreiter

Graz, 17.6.2015

Eidesstattliche Erklärung

Ich erkläre ehrenwörtlich, dass ich die vorliegende Arbeit selbstständig und ohne fremde Hilfe verfasst habe, andere als die angegebenen Quellen nicht verwendet habe und die den benutzten Quellen wörtlich oder inhaltlich entnommenen Stellen als solche kenntlich gemacht habe.

Graz, am 17.6.2015 *Anna Müller eh*

Acknowledgments

I am very grateful to my supervisors Univ.-Prof. Dr.med.univ. Peter Wolf and Priv.-Doz.in Dr.in med.univ. Ariane Aigelsreiter, who assumed supervision of my diploma thesis and who took a lot of time to provide helpful guidance. Further I would like to thank Univ.-Prof. Dr.med.univ. Werner Aberer and Univ.-Prof. Dr.med. Dr.med.habil. Jürgen Christian Becker, PhD for their advice.

A special thanks goes to all the staff of the Oncogenomics lab at the QIMR Berghofer Medical Research Institute in Brisbane who supervised me in the lab and helped out with any questions. In particular I would like to thank Professor David Whiteman B Med Sci, MBBS (Hons) PhD FAFPHM, Professor Nicholas Hayward, PhD, Dr. Elke Hacker, PhD, Thomas Pollak, Mitchell Stark, PhD, Professor Clay Winterford and Glynn Rees.

I am also very thankful to Dipl.-Ing. Georg Wehowar for the help and time invested for the statistical analysis.

I would also like to thank the Medical University of Graz for the financial support in form of a research scholarship.

Last but not least I am very grateful for all the support from my family and my colleague Gregor Mayer, without whom this project would not have been possible.

Zusammenfassung

Einleitung: Das maligne Melanom ist der sechsthäufigste maligne Tumor der westlichen Welt mit einer steigenden Inzidenzrate von 4-6% pro Jahr. Etwa 50% aller Melanome zeigen eine V600E-Mutation des für das BRAF-Protein kodierenden Protoonkogens. Patienten mit einem Melanom, die diese Mutation aufweisen, können im Sinne einer „targeted therapy" mittels BRAF-Inhibitoren (z.B. Vemurafenib oder Dabrafenib) im metastasierenden Stadium effektiver therapiert werden als mit einer Chemotherapie (z.B. Dacarbazin). Die klinische Relevanz dieser Forschung begründet sich im Bedarf einer personalisierten Medikation für betroffene Patienten. Ziel war es, den Anteil der Zellen mit einer V600E-Mutation in Melanomengeweben zu quantifizieren.

Methoden: 62 Melanomproben wurden mithilfe eines mutationsspezifischen Antikörpers (VE1), welcher BRAF-V600E-mutierte Zellen mit hoher Spezifität und Sensitivität darstellt, immunhistochemisch analysiert. Nach händischer Optimierung der immunhistochemischen Färbemethoden wurde der Farbstoff Nova Red für alle Proben zur Färbung verwendet; 31 der Proben wurden zusätzlich mit dem Farbstoff Vina Green gefärbt. Anschließend wurden von den immunhistochemisch gefärbten Schnitten mittels eines in ein Mikroskop (Aperio XT ScanScope) integrierten Kamerasystems Aufnahmen gemacht. Diese wurden sowohl visuell als auch mittels der Bildanalysesoftware Aperio ImageScope mit dem Ziel, einen Algorithmus für die Quantifizierung der BRAF-Expression im Melanomgewebe zu erstellen, ausgewertet. Um die Ergebnisse der beschriebenen Färbemethode zu validieren, wurden 13 der immunhistochemisch gefärbten Proben mit der Restriktionsverdauungsmethode auf das Vorhandensein einer BRAF-V600E-Mutation getestet. Weiters wurden die Ergebnisse mit bestehenden Genotypisierungsdaten, ermittelt durch MALDI-TOF (Goldstandard), verglichen.

Ergebnisse: Mit MALDI-TOF zeigten sich 18 der 62 (29%) Proben positiv auf die BRAF-V600E-Mutation. Die visuelle Auswertung der Immunhistochemie ergab, dass 15 der 62 (24%) Proben mit dem Farbstoff Nova Red und 2 der 31 (6%) mit Vina Green positiv waren. Verglichen mit der MALDI-TOF-Methode (als Goldstandard) zeigte die Nova Red-Auswertung eine Sensitivität von 66,7% und eine Spezifität von 93,1%. Cohens Kappa betrug 0,63 (95% CI, 0,41 - 0,85) mit einem p-Wert von 0,000000589. Die Vina Green-Auswertung hatte eine Sensitivität von 100% und eine Spezifität von 33,3%. Cohens Kappa betrug 0,45 (95% CI, 0,02 - 0,87) mit einem p-Wert 0,00284. Die computergestützte Auswertung der immunhistochemischen Färbungen zeigte höhere Medianwerte der

Positivität (Prozentzahl der positiven Pixel im gesamten ausgewerteten Feld einer Probe) bei Proben mit einer V600E-Mutation am BRAF-Gen als bei Proben ohne Mutation.

Schlussfolgerung: Sowohl die immunhistochemische Färbemethode mit visueller bzw. mit computergestützter Auswertung als auch die Restriktionsverdauungsmethode war der genetischen Methode mit MALDI-TOF im Nachweis von BRAF-V600E-Positivität unterlegen. Daher bleibt MALDI-TOF der Goldstandard im Nachweis von BRAF-V600E-Positivität als Voraussetzung für eine BRAF-Inhibitor-Therapie.

Schlagwörter: Malignes Melanom, BRAF-V600E-Mutation, Immunhistochemie, VE1-Antikörper, Genotypisierung, Restriktionsverdauungsmethode, MALDI-TOF-Methode

Declaration

The work carried out to gain the data for the immunohistochemical analysis (both for the visual and computer-aided evaluation) and the analysis itself was done by me. I received helpful advice and an introduction to the lab work by Thomas Pollak throughout the project. Further all practical work and analysis concerning the Restriction Digest Method was carried out by me. An introduction to and advice concerning this method was given to me by Mitchell Stark, PhD.

All work concerning the acquisition of data by genotyping with MALDI-TOF was not carried out by me but the data was kindly supplied by the work group of Professor David Whiteman and Dr. Elke Hacker.

Statistical analysis was carried out in collaboration with Dipl.-Ing. Georg Wehowar.

Abstract

Introduction: Malignant melanoma is the sixth most diagnosed cancer and has a yearly increase in incidence of 4 to 6% in fair skinned populations in the western world. Approximately 50% of all melanoma carry a V600E mutation on the BRAF gene. Melanoma patients in advanced tumour stages with this specific mutation are eligible for targeted therapy with BRAF-inhibitors, such as Vemurafenib and Dabrafenib, instead of conventional chemotherapy with Dacarbazin. The clinical relevance of this research is based on the need for specific treatment of patients in terms of personalised medicine. The goal was to quantify the amount of cells carrying a V600E mutation in malignant melanoma tissue.

Methods: 62 melanoma samples were analysed by the means of immunohistochemistry with a mutation specific antibody (VE1) that detects BRAF V600E mutated cells with high specificity and sensitivity. After optimisation of immunohistochemical staining methods "on the bench" the chromogen Nova Red was used in all samples; 31 of the samples were additionally stained with the chromogen Vina Green. Subsequently, images were taken of the immunohistochemically stained samples with a camera system integrated in a microscope (Aperio XT ScanScope). Visual examination was performed and with the help of an image analysis software (Aperio ImageScope) an attempt was made to create an algorithm for the quantification of the BRAF expression in melanoma. To validate the results obtained by immunohistochemistry, 13 samples were tested with genotyping by restriction digest method. Further, the results of immunohistochemistry and restriction digest were compared to results produced by genotyping with MALDI-TOF as the gold standard.

Results: MALDI-TOF found 18 of the 62 (29%) samples to be positive for the V600E mutation. By visual evaluation of immunohistochemistry 15 of 62 (24%) were positive with Nova Red but only 2 of 31 (6%) with Vina Green. Compared to MALDI-TOF, immunohistochemistry with Nova Red showed a sensitivity of 66,7% and a specificity of 93,1%. The calculation of Cohen's Kappa resulted in kappa=0,63 (95% CI, 0,41 to 0,85) with a p-value of 0,000000589. Immunohistochemistry with Vina Green on the other hand had a sensitivity of 100%, a specificity of 33,3% and a Cohen's Kappa of 0,45 (95% CI, 0,02 to 0,87) with a p-value of 0,00284. Computer-aided evaluation of immunohistochemical stains produced higher median „positivity values" (percentage of positive pixels per total area analysed) in BRAF V600E positive samples than in negative ones.

Conclusion: In our hands, immunohistochemistry with visual or computer-aided evaluation and the restriction digest method were inferior to the genetic method of MALDI-TOF in detecting BRAF V600E mutations in melanoma samples. Thus MALDI-TOF remains the gold standard to detect this specific BRAF mutation as a prerequisite for BRAF-inhibitor treatment.

Key words: Malignant Melanoma, BRAF V600E Mutation, Immunohistochemistry, VE1 Antibody, Genotyping, Restriction Digest Method, MALDI-TOF

Contents

Glossary and List of Abbreviations

Genes and Proteins

BRAF	B-Raf proto-oncogene, serine/threonine kinase
CDK4	cyclin-dependent kinase 4
CDKN2A	cyclin-dependent kinase inhibitor 2A
P14ARF	= CDKN2A
CDKN2B	cyclin-dependent kinase inhibitor 2B
MCR1	melanocortin-1-receptor (alpha melanocyte stimulating hormone receptor)
PI3-Kinase	phosphoinositide-3-kinase (skin-derived)
MAP-Kinase	mitogen-activated protein kinase
AKT	v-akt murine thymoma viral oncogene
PTEN	phosphatase and tensin homolog
mTOR	mechanistic target of rapamycin (serine/threonine kinase)
ERK	extracellular signal-regulated kinases (same as MAPK1)
MITF	microphthalmia-associated transcription factor
RTK	receptor tyrosine kinase
GPB2	growth factor receptor binding protein 2
NRAS	neuroblastoma rat sarcoma viral oncogene homolog
HRAS	harvey oncogene homolog
KRAS	kirsten rat sarcoma viral oncogene homolog
SOS	son of sevenless protein homolog
MAPKK	mitogen activated protein kinase kinase
MEK	= MAPKK
c-Myc	c-Myc avian myelocytomatosis viral oncogene homolog
ELK 1	ELK1, member of ETS oncogene family
c-Fos	FBJ murine osteosarcoma viral oncogene homolog
GAP	GTPase activating protein
HMB-45	human melanoma black-45 monoclonal antibody
MART-1	melanoma antigen recognized by T cells 1 (protein)

Other

RR	relative risk
CI	confidence interval
GTP	guanosine triphosphate
LMM	lentigo maligna melanoma
TNM	classification of malignant tumours
AJCC	American Joint Committee on Cancer
CT	computer tomography

PET	positron emission tomography
MRT	magnetic resonance imaging
PCR	polymerase chain reaction
IHC	immunohistochemistry
HRM	high resolution melting analysis
SLND	sentinel lymph node dissection
Fc	fragment constant
Fab	fragment antibody-binding
HRP	horseradish peroxidase
AP	alkaline phosphatase
PIER	proteolytic induced epitope retrieval
HIER	heat induced epitope retrieval
AB	antibody
RT	room temperature
TBS	tris-buffered saline
dNTPs	desoxyribonukleoside triphosphates

List of Figures

List of Tables

1 Introduction

1.1 Aim of the Study

Cutaneous melanoma and the research on this topic is of growing interest to medical staff and society in general due to its rising occurrence not only in highly sun exposed countries, such as Australia and New Zealand, but also in central Europe and the US (5). The finding that malignant melanoma often carry somatic mutations in the BRAF gene, which promotes melanoma growth, gave rise to new treatment options and hence a concept of personalised targeted treatments for patients with metastatic melanomas carrying the BRAF mutation has been established (6).

The goal of this project was to find a cost efficient method for identifying malignant melanoma with a BRAF V600E mutation to use for pre-screening and research.

H_0 = The BRAF V600E mutation cannot be identified with immunohistochemical methods in malignant melanoma.

H_1 = The BRAF V600E mutation can be identified with immunohistochemical methods by evaluation under the microscope and/or by computer-aided evaluation.

1.2 Melanoma

1.2.1 Definition

Cutaneous melanoma is defined as cancer evolving from the pigment producing cells of the skin (7, 8).

1.2.2 Epidemiology

Incidence and Mortality

Over the past decades, the melanoma incidence rate has increased rapidly and is still on the rise. In fair skinned populations all around the world an increase of at least 4 to 6% per year has been registered in the age-standardized incidence rates. It has risen faster than any other type of cancer and is currently the sixth most diagnosed type of cancer in the US in both males and females. The incidence rate is generally higher in fair skinned rather than darker skinned individuals (5, 7).

Age & Gender Differences

Individuals suffering from melanoma are predominantly of young age with a median of 52 years - thus nearly ten years younger than the point in life, when most other tumours strike (e.g. colon, lung and breast) (5, 7).

According to Liu et al. there is a significant difference in the incidence of melanoma between males and females. It was shown that up to the age of 44, females are more prone to getting cutaneous melanoma, while at ages over 44, men had a higher risk (9).

Geographical Variation

According to a study by Crombie, the melanoma incidence rate increases as latitude decreases, which is explained by the decreasing UV radiation at higher latitudes. The latitude hypothesis is inversed in Europe, which is explained by the higher density of skin pigmentation in populations living in southern Europe as the stronger pigmentation acts as a protective factor in melanoma development (7, 10).

Risk Factors

Major risk factors for melanoma development include: five or more atypical naevi, the number of banal melanocytic naevi, red hair colour, sunburns in childhood and adulthood, atypical naevi and chronic sun exposure (11).

Environmental Factors

UV light has been shown to be an environmental factor, which has an impact on the development of cutaneous melanoma (11). Others argue that UV light only has an impact on melanoma development during specific periods in an individual's life (e.g. childhood). Autier et al. showed that fair skinned immigrants from regions with high UV exposure (e.g. Africa) to regions with lower UV exposure (Northern Europe) still had a very high risk of developing melanoma (7, 12).

Genetic Factors

Around 10% of individuals suffering from melanoma show a familial melanoma history (7).

Prognostic Factors

Tumour thickness is the most important factor concerning prognosis in melanoma. The thicker, the more likely it is for it to metastasize both via the bloodstream and the lymphatic system. Hence the Breslow thickness (in millimetres) is a good value for determining

prognosis. Further the nodal status is a measure for survival, especially in patients, who first presented with a node negative primary melanoma (13).

In localized invasive malignant melanomas (stage I and II) BRAF, NRAS and KIT mutations are indicators for a poorer disease-free survival and overall survival (14).

1.2.3 Aetiology and Pathogenesis

Cancer cells replicate frequently. Even though melanocytes have "dormant" phases, they divide periodically and are therefore prone to turn into fast dividing malignant cells (7).

It has been shown, that the progression from healthy to malignant cells is a step-by-step act. Associated with that are several accumulating genetic mutations, which can be visualised by histologic changes to the cells: melanocytic atypia, atypical melanocytic hyperplasia, radial growth phase melanoma, vertical growth phase melanoma, metastatic melanoma (15).

Melanoma are only seen to evolve very rarely from pre-existing naevi. More often they arise from healthy melanocytes just by a different pathway than naevi. Various pathways involving molecular genetic events have been found to produce malignant melanoma cells. These events include translocation, amplification, deletion and point mutations on DNA level (16).

Two genes are mainly linked to familial melanoma development and are classified as high risk genes: *CDKN2A* and *CDK4*. These encode for proteins which act as tumour suppressors by influencing the cell cycle arrest. Other genes linked to melanoma development are part of cancer syndromes such as Xeroderma pigmentosum (DNA repair gene is impaired), Retinoblastoma, Li Fraumeni, etc. (7, 11, 17).

The best known "low risk gene" for melanoma development is the melanocortin-1-receptor gene (MCR1), which is also associated with the somatic BRAF mutation. The prevalence is 50% among the European population. Phenotypically red hair and freckles occur (5, 7, 17).

Somatic chromosome changes have shown to impact melanoma development. In the last 20 years the BRAF mutation has been subject to a lot of research. The gene can be found in 40 – 60% of all melanomas and codes for a serine/threonine kinase, which is part of the MAP-Kinase pathway. A higher amount of kinase activity is present when mutated (18, 19).

As the BRAF V600E gene mutation leads to a changed BRAF protein, which again plays a major role in this MAP-Kinase pathway, a detailed description follows:

MAP-Kinase Pathway

This pathway is hyperactivated in melanoma cells with mutations on the NRAS or BRAF genes. This leads to hyperphosphorylation of the following MEK and ERK proteins which again causes the release of a big amount of transcription factors (MITF), leading to cell proliferation and survival of the cancer cells (20).

The pathway starts off with a membrane bound receptor of the receptor-tyrosine-kinase family (RTK receptor). When a ligand binds, two subunits of the RTK receptor dimerise. Domains on the inside of the receptor catalyse autophosphorylation and phosphorylation of the other subunit. Next Growth factor receptor binding protein 2 (GPB2) binds to the phosphorylated RTK leading to the SOS protein binding to the GPB2. Then the RAS protein binds to the SOS protein together with a GDP. Due to the SOS, the GDP can be exchanged with a GTP and thus the RAS is activated. In its active state, the RAS protein can bind to various effector proteins, one of them being the BRAF protein. Studies have shown, that BRAF is most susceptible for RAS to bind (21). Activated RAF-Kinase activates and phosphorylates MEK 1 and 2, which in turn activates and phosphorylates ERK 1 and 2. MEK (MAPKK) and ERK (MAPK) are kinase enzymes as well. The activated ERK protein can trigger many different reactions, two very important ones will be described as follows: First of all, it can activate the transcription factor c-Myc by phosphorylation. Secondly, ERK can activate the transcription factor ELK 1 by phosphorylation, which in turn binds to a promoter region on the DNA and leads to the transcription of the c-FOS gene by enhancing the affinity of the DNA to RNA polymerases. c-FOS dimerises with the c-JUN protein, building another transcription factor: FOS-JUN. Both the c-Myc and the FOS-JUN transcription factors bind to promoter regions triggering the formation of Cyclin D, proteins for replication, cytokines, etc. As a consequence, cell proliferation is stimulated. In a healthy cell, the MAP-Kinase is turned off by a GTPase activating protein (GAP) binding to the RAS-GTP complex. The GAP protein hydrolyses the GTP to GDP, leading to a dissociation of the RAS. If the RAS protein is mutated though, it cannot be activated as the GAP protein is not able to dephosphorylate GTP to GDP. Thus the BRAF protein stays activated and the whole cascade is not “turned off” leading to uncontrolled proliferation (18, 22-24).

The BRAF V600E mutation gives rise to the activation of the MAP-Kinase and further causes insensitivity to negative feedback mechanisms (18).

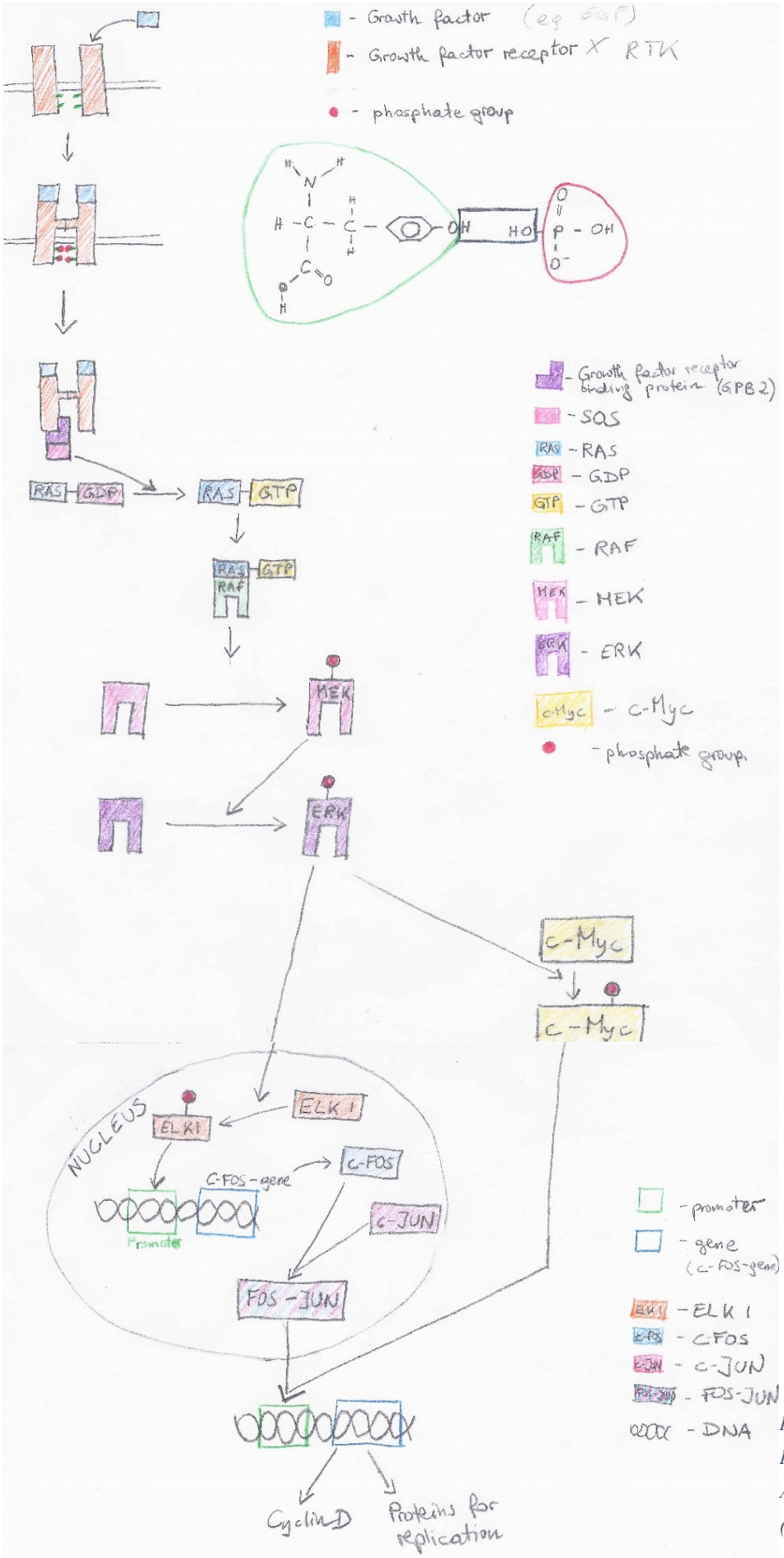

Figure 1 The MAP-Kinase Pathway - Redrawn and Adapted from Cited Video (1-3)

BRAF

Around 50% of all melanoma carry a somatic mutation of the BRAF gene, which is located on chromosome 7q34 (18, 19, 25). Most of the BRAF mutations occur as a point mutation, exchanging tyrosine with an adenosine, thus replacing the amino acid valine by glutamate. This specific mutation is known as the V600E mutation of the BRAF gene (20). It was found that the basal kinase activity of BRAF is higher than that of other RAF-family-members, which is why BRAF mutations occur quite frequently in various tumours (21, 26). BRAF mutations can be found in different kinds of internal cancers (colon, thyroid) and in mucosal melanoma, thus cancers on non-sun-exposed sites. This leads to the concept that the mutation is not necessarily caused by sun exposure. Oxidative damage in general could lead to a BRAF V600E mutation (11). On the other hand, melanomas with BRAF mutations have been more often found on sites, which were intermittently, rather than chronically exposed to the sun. Therefore the mechanisms behind this mutation are not yet fully understood. Others argue, that a mutation of the BRAF gene is an early-life-event, as many benign or dysplastic naevi also carry a mutation on that gene locus (20).

As described above, the BRAF protein is a serine/threonine protein kinase and is involved in the stimulation of the ERK pathway. It is activated by the NRAS protein and its job is the transmission of signals from surface receptors to the nucleus (27). The BRAF protein has no influence on the PI3K pathway but some association between activated BRAF mutations and PTEN deletions were observed. This leads to the hypothesis that both the MAPK pathway and the PI3K pathway need to be stimulated at the same time for a melanoma to evolve. Further evidence that BRAF V600E mutation by itself is not a triggering factor for melanoma development was shown by Fisher et al., as the mutation of the BRAF gene only lead to the evolvement of a benign nevus whereas BRAF mutation plus p53 deficiency enhanced melanoma development (20).

PI3-Kinase Pathway

This pathway is hyperactivated in melanoma cells due to the loss of a tumour suppressor gene (PTEN). This causes the phosphorylation and hence activation of AKT, a survival gene. Thus the mitogenic mTOR pathway is activated which results in melanoma cell growth (20).

1.2.4 Classification

Superficial spreading melanoma embraces around 70% of all types. It has been associated with high amounts of UV radiation and is often found on extremities and the trunk (27, 28).

Nodular melanoma accounts for 20% of all melanoma types and has no preceding horizontal growth phase but jumps straight to the vertical. Thus they are often diagnosed very late, leading to poor prognosis (27, 28).

Lentigo maligna melanoma makes up 10-20% of all melanoma. They often occur in elderly people on chronically sun damaged skin (face, etc.). LMMs are usually very slow growing and have a prolonged horizontal growth phase before entering vertical growth (27, 28).

Acral lentiginous melanoma are very rarely found (<5%). The aetiology does not seem to be connected to UV radiation. Usually they are spotted as a mucosal melanoma or on the acres (palmar, plantar, subungual) (27, 28).

TNM Classification (Table 1 and 2)

The most widely used classification for any cancer is the TNM Classification (AJCC Version of 2009) (29). Specifically for melanoma, the T represents tumour thickness, mitotic rate and ulceration. N stands for the number of lymph nodes affected. M describes the site of distant metastasis and the serum lactate dehydrogenase level (27, 28).

T Classification	Thickness	Ulceration Status
Tis	NA	NA
T1	≤1.0 mm	a: w/o ulceration and mitosis < 1/mm^2 b: with ulceration or mitosis ≥1/mm^2
T2	1.01-2.0 mm	a: w/o ulceration / b: with ulceration
T3	2.01-4.0 mm	a: w/o ulceration / b: with ulceration
T4	>4.0 mm	a: w/o ulceration / b: with ulceration
N Classifications	No. of Metastatic Nodes	Nodal Metastatic Burden
N0	0	NA
N1	1	a: micrometastasis / b: macrometastasis
N2	2-3	a: micrometastasis b: macrometastasis c: in-transit metastasis/satellite(s) w/o metastatic nodes
N3	4+ metastatic nodes, or matted nodes, or in-transit metastases/satellites with metastatic nodes	
M Classification	Site	Serum LDH
M0	No distant metastases	NA
M1a	Distant skin, subcutaneous, or nodal metastases	Normal
M1b	Lung metastases	Normal
M1c	All other visceral metastases Any distant metastases	Normal Elevated

Table 1 AJCC (2009) - TNM Classification of Malignant Melanoma – Adapted from (29)

Clinical Staging				Pathological Staging			
Stage 0	Tis	N0	M0	Stage 0	Tis	N0	M0
Stage IA	T1a	N0	M0	Stage IA	T1a	N0	M0
Stage IB	T1b	N0	M0	Stage IB	T1b	N0	M0
	T2a	N0	M0		T2a	N0	M0
Stage IIA	T2b	N0	M0	Stage IIA	T2b	N0	M0
	T3a	N0	M0		T3a	N0	M0
Stage IIB	T3b	N0	M0	Stage IIB	T3b	N0	M0
	T4a	N0	M0		T4a	N0	M0
Stage IIC	T4b	N0	M0	Stage IIC	T4b	N0	M0
Stage III	Any T	≥N1	M0	Stage IIIA	T1-T4a	N1a	M0
					T1-T4a	N2a	M0
				Stage IIIB	T1-T4b	N1a	M0
					T1-T4b	N2a	M0
					T1-T4a	N1b	M0
					T1-T4a	N2b	M0
					T1-T4a	N2c	M0
				Stage IIIC	T1-T4b	N1b	M0
					T1-T4b	N2b	M0
					T1-T4b	N2c	M0
					Any T	N3	M0
Stage IV	Any T	Any N	M1	Stage IV	Any T	Any N	M1

Table 2 Staging of Malignant Melanoma – Adapted from (29)

1.2.5 Diagnostics

Symptoms

Most cutaneous melanoma occur symptom-free. These often only arise in advanced tumour stages. Bleeding, pain or ulceration of the lesion may indicate high tumour progression (28).

If the tumour has already metastasised lymphogenically, the spreading may be seen in the form of black spots around the primary lesion (satellite metastasis) or between the primary lesion and the lymph nodes (in-transit metastases). In the case of distant metastasis, the tumour spreads haematogenically which leads to disseminated elevations of the skin. Melanin may circulate in the bloodstream, which leads to melanocytosis leaving the patient with a blue-grey tan (30, 31).

General Diagnostics

Around half of the melanoma are spotted by the patients or their family members. Therefore self-examination is one of the most effective, easiest, inexpensive and non-invasive ways of detection and prevention, if carried out carefully and regularly (15, 28).

The whole skin surface, nails and eyes are to be checked regularly by a dermatologist. Naked eye inspection of the skin has mostly been replaced by dermoscopy as the latter method has been proven to improve diagnosis (32, 33).

The ABCD rule of dermoscopy is most commonly used to assess a pigmented lesion:

ABCD-Scheme: A – asymmetry
B – border irregularity
C – colour variation (shades of brown, black, blue, red and white)
D – diameter > 5 mm (28, 34)

But also a change in elevation, surface texture, appearance of the surrounding skin, etc. can accompany the evolvement of cutaneous melanoma (15).

Very often melanomas lack one or more of these obvious criteria and are hence more difficult to diagnose. Sometimes individuals have a few odd naevi and thus the "ugly duckling" scheme is more standing to reason. This method suggests to compare the individual naevi of a single person among one another and inspect the "odd ones" carefully (35).

To check for tumour spreading, a chest X-Ray, an ultrasound of the abdomen, a CT and PET examination of the thorax and the abdomen as well as a CT or MRT of the brain can be carried out (31).

Histological Examination

The definite diagnosis is made by assessing the biopsy material under the microscope. The tissues is usually conserved by either cryoconservation or with paraffin, thinly cut, fixed on a slide, stained and inspected with a light microscope. The histopathological diagnosis is posed by assessing the cytological and architectural microscopic features. The main points pathologists determine concerning the architecture are: large dimensions, asymmetry and poor circumscription, predominance of single melanocytes, extensive involvement of adnexal epithelium by atypical melanocytes, presence of atypical melanocytes throughout entire thickness of the epidermis and irregularity in size and shape of nests of melanocytes. Each melanoma subtype has its specific cellular and architectural hints (13).

As shown in the TNM Classification, the main predictors for survival are tumour thickness, nodal status and tumour ulceration.

Tumour thickness is represented by the Clark-Level, which is shown in Table 3, or the Breslow-Index.

Clark-Level	Depth of Tumour Invasion
I	Tumour cells confined to epidermis
II	Tumour cells penetrate into papillary dermis
III	Tumour cells fill papillary dermis
IV	Tumour cells extend into reticular dermis
V	Tumour cells invade subcutis

Table 3 Clark Level – Adapted from (36)

The Breslow Index is defined as the invasion depth of the tumour cells measured in millimetres. Breslow arranged the depth into five sections. This index is nowadays replaced by the T in the TNM Classification with slightly different numbers as in the original Breslow Index (36).

Laboratory Testing / Laboratory Parameters

If the diagnosis of cutaneous melanoma is unsure or for specific therapy, the biopsy material may undergo different laboratory tests.

Immunohistochemical markers for melanocytic lesions are the S100 protein or testing with an antigen-cocktail comprised of HMB-45, MART-1 and tyrosinase (16).

Due to the fact that roughly 50% of all melanoma carry a mutation on the BRAF gene (of which 70-90% are positive for BRAFV600E mutation) (19) and there being specific medication (Vemurafenib) available if positivity is proven, melanoma excisions are usually tested for this mutation. Different methods for testing this mutation are available for clinical therapeutic use, among which directional Sanger sequencing of PCR products, pyrosequencing and next generation sequencing can be found.

Genotyping is the means of choice before prescribing targeted therapy as it is the most established method in the clinical setting. It was therefore also used as the gold standard in this experiment (37). Immunohistochemistry with VE1 antibody is applicable in research only.

1.2.6 Treatment

Surgical Therapy

The main treatment of cutaneous melanoma is surgical. Depending on tumour thickness, different excision margins are applied (Table 4).

Thickness of Tumour	Excision margin
Melanoma in situ	5 mm
< 2,0 mm	10 mm
≥ 2,0 mm	20 mm

Table 4 Excision Margin Guidelines for Malignant Melanoma – Adapted from (8)

Sentinel lymph node dissection (SLND) is state of the art for patients with melanoma thickness ≥1 mm. If the SLND is positive in terms of showing metastases, radical lymph node dissection is recommended. Skin metastases are usually treated surgically, but if multiple occur, other treatments can be considered (8).

Radiation

Radiation therapy of the primary tumour is only indicated, if surgery has already become impossible or the region is difficult to operate on, such as the face. Sometimes it is applied in lentigo maligna melanoma, or in elderly people.

Affected lymph nodes and in-transit metastases are sometimes exposed to radiation therapy, if surgical treatment is impossible. Bone and brain metastases can be effectively treated with radiation, leading to pain reduction and prolongation of survival (8).

Medical Therapy

Adjuvant Therapy

Adjuvant interferon therapy is advised in patients with a cutaneous melanoma of stages IIB – IIIC (38). It seems to improve the disease free and overall survival (8).

Chemotherapy

Its indication is generally inoperability or recurrence of the primary tumour, inoperable regional metastases or distant metastases. Therefore, this often affects palliative patients, for whom this leads to prolongation of survival or minimisation of symptoms/reduction of tumour size. The most commonly used single-agent chemotherapy are Dacarzabine, IL-2 and INF leading to tumour remission between 5 and 12%. Polychemotherapy is very rarely used due to its high toxicity (8).

Targeted Therapy/Personalised Medicine

In 2012, the first targeted therapy as a first-line treatment against metastasised melanoma with the BRAF V600E mutation was licensed: Vemurafenib. It is a selective adenosine triphosphate competitive antagonist of the V600E mutant BRAF serine/threonine kinase. In the phase 1 trial, a maximum dosage of 960 mg twice daily was found to work best. In phase 2 it was shown, that there is tumour regression in the early treatment phase. This phase is followed by disease stabilization for around six months, then progression of the tumour started again. The drug had a response duration of 2-18 months. Phase 3 compared Vemurafenib to the official first line drug Dacarbazine. A relative reduction of 63% in the risk of death and 74% in the risk of either death or disease progression compared with Dacarbazine was shown. Phase 4 confirms the safety of the drug (39, 40).

The overall response rate was 53%, of which 6% had a complete response while 47% had a partial response (41). Dose escalation was registered at 1120 mg twice daily.

Adverse effects are quite common, and arise more often in elderly patients over 75 years of age (42). The events include: rash, arthralgia, fatigue, photosensitivity, alopecia and nausea in descending order of frequency (43). Moreover, the response of individual patients is quite variable to BRAF inhibitor treatments (6). As an alternative to Vemurafenib the drug Dabrafenib can be given, which also acts as a BRAF inhibitor (44).

It has been found that after a median of 5,8 months, patients become resistant to BRAF inhibitors when given as monotherapy. Various different pathways for becoming resistant have been identified. The BRAF-inhibitor paradox explains that these inhibitors only inhibit monomeric BRAF signalling and enhance dimeric RAF signalling. Thus all cells with the ability to upregulate dimeric MAPK pathway signalling may use this advantage in terms of growth. Other neoplasms such as colorectal cancer and squamous cell carcinomas have been associated with Vemurafenib. The paradoxical activation of the MEK pathway may also occur through upstream RAS signalling (39, 45-47).

In order to prolong the progression-free survival, a combination of the BRAF inhibitor Dabrafenib and the MEK inhibitor (=MAPK kinase inhibitor) Trametinib is now given to patients. This has led to a median progression-free survival of 9,4 months when each was given at its single agent dose (47).

As can be seen in Figure 2, there are several different drugs which target the MAPK pathway, but due to the formation of resistance, Arkenau et al. suggest that a combination of therapies attacking different pathways (e.g. RAS-RAF-MEK-ERK or PI3K-AKT-mTOR) may be more effective in the future than monotherapies (48, 49).

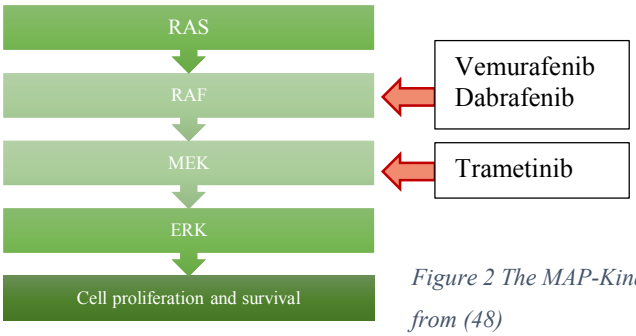

Figure 2 The MAP-Kinase Signalling Pathway and Targeted Drugs – Adapted from (48)

Immunotherapy

Another approach comprises the stimulation of the immune system to work against cancer cells. A drug attempting this theory is Ipilimumab, a monoclonal antibody. CTLA-4 (cytotoxic T-lymphocyte antigen-4 is a molecule) is expressed on the surface of activated cytotoxic T cells. Ipilimumab blocks this molecule which results in a better outcome in increased survival of the melanoma patients (50, 51).

2 Materials and Methods

2.1 Immunohistochemistry

The main essence of immunohistochemistry is the interaction between an antigen and an antibody according to the lock-and-key model. Ideally a specific and strong binding between the antibody and the epitope takes place. A detection system is attached to the antibody, in order to make it visible (52).

Antigens consist of several different epitopes. An epitope is an amino acid sequence which makes up a specific three-dimensional structure for an antibody to fit. These epitopes can be found on the cell surface, in the nucleus or the cytoplasm (52).

Firstly, the specific antibody needs to be produced. This happens by introducing a macromolecular antigen into a laboratory animal, such as a rat, goat, mouse or rabbit by injecting the antigen concentrate subcutaneously. The organism of the animal reacts to the foreign substance by producing antibodies to the diverse epitopes of the substance. Thus this leads to polyclonal antibody production, as they are not all directed against the same epitope and are produced by different stem cells of the blood serum. Repetitive immunisation with the antigen concentrate is called boosting. In order to produce monoclonal antibodies which are directed against only one epitope, the antigen is introduced into a single "immortal" myeloma cell and after boosting, antibodies are harvested (52, 53).

An antibody consists of a Fragment constant (Fc) and a Fragment Antibody-binding (Fab). For immunohistochemistry, the Fab is modelled to fit the Epitope. Each half of the antibody, if split lengthwise, consists of a heavy (γ) and a light chain (κ or λ). Cross-reactions seem to be very common and staining always needs to be looked at and interpreted carefully (52-54).

For this specific experiment, there were two different antibodies to choose for detecting the V600E mutation: the Antibody against the VE1 mutation or the anti-B-Raf. According to literature, the first one has a higher sensitivity and specificity (55). Thus it was chosen for this experiment.

Antigen – antibody binding is based on hydrogen bonds, electrostatic adhesion and Van-der-Waal forces. An equilibrium is formed between bonded and non-bonded antibodies. High affinity leads to requiring smaller antibody concentrations, faster binding to the antigen and stronger binding. The antibody concentration, incubation time and temperature are in close relation to one another. If one is changed, the others adjust. Generally speaking, the higher

the concentration, the faster the reaction but the likelihood of unspecific bindings rises at the same time. Higher temperatures lead to faster reactions too (52, 56).

In the majority of cases, the antibodies are tagged with enzymes, which convert chromogens into stain. Horseradish peroxidase (HRP) and alkaline phosphatase (AP) are the most frequently used enzymes. Due to the fact, that most tissues contain endogenous peroxidases or phosphatases, these need to be blocked which will be described later on. Instead of enzymes the antibodies can also be tagged with fluorochromes, biotins or other chemicals. For horseradish peroxidase, the iron-containing haem-group reacts with the hydrogen peroxide to form a complex, which again degenerates to water and oxygen and the enzyme is freed again. The electrons required for this reaction come from the chromogen, which in turn is oxidised leading to visible stain. Alkaline phosphatase on the other hand hydrolyses an organic phosphate. The product reacts with the chromogen to produce colourful stain. For enhancement, enzyme-conjugated polymers can be attached to the antibodies. This leads to more chromogens being able to bind to the antibody and thus results in stronger staining, even if only few antigens are present. Therefore this methods increases the sensitivity (52).

For IHC to work, the paraffin wax, which has been used to preserve the biopsy material, to be able to cut the specimen and fix it onto a slide, now needs to be removed. Deparaffinising is carried out with the chemical Xylol or a substitute for at least 20 minutes. Subsequently, the tissue is "rehydrated" in a descending alcohol series ending up in aqua dest. - the exact opposite to what has happened when fixation of the tissue to the slide was done (ascending alcohol series) (52).

Next antigen-demasking/antigen-retrieval needs to be accomplished. The epitopes have been covered/changed due to the fixing and preserving of the tissue. Formaldehyde, a preservative, frequently reacts with epitopes containing lysine-, cysteine- and arginine-residues. Due to these reactions methylol groups, Schiff bases and methylene bridges evolve (52, 54).

Antigen-demasking can either be done using proteolytic enzymes (PIER) or heat (HIER). For PIER (proteolytic induced epitope retrieval) Proteases (0,1%) and Trypsin (0,05%) are solved in a buffer solution and applied to the tissue between 15 and 40 minutes at room temperature or 37°C. Heat induced epitope retrieval (HIER) is accomplished by applying heat (100°C) and humidity at a pH of 2-10. This leads to epitopes being exposed and available for antibody binding. The time of the specimen being exposed to this procedure and the temperature are directly proportional. Thus, the longer the time interval, the lower

the heat and vice versa. Epitope retrieval solutions can be bought as a whole or prepared from citrate buffer (pH 6), EDTA solution (pH 8) or Tris EDTA (pH 9,9 or 10). In order to ensure constant heat exposure for standardised protocols, decloaking chambers (modified pressure cookers) are used. The time required to cool the slides slowly after HIER is included in the time stated as the retrieval time. Instead of a decloaking chambers, protocols have also been developed using microwaves, water baths, steam cookers or autoclaves (52).

After epitope retrieval, the antigen – antibody reaction is induced. There are different kinds of methods (direct and indirect methods). In the direct method a fluorochrome is directly linked to the primary antibody. This is therefore a simple and fast method for detecting epitopes. In order to ensure, that the signal is actually from an antibody binding to an epitope, negative and positive controls should be included. Negative controls: incubating the slide with the rinsing buffer or the marked serum only. Further a slide which is for sure positive and one for sure negative should be included in each run. One disadvantage of this method is that the sensitivity can be quite low. Further tagging an antibody directly with a fluorochrome can lead to affinity loss to the antigen. In order to increase the sensitivity, polymers are sometimes linked to the primary antibody. This polymer can hold a greater number of fluorochromes and therefore the signal is stronger. In the indirect method the tissue is incubated with an untagged primary antibody. Thereafter another antibody tagged with a fluorochrome and directed against the first antibody is applied. As several secondary antibodies can bind to one primary, this leads to an amplification of the signal and therefore an increase in sensitivity of the method. Sometimes enzymes are connected to the primary antibody instead of a fluorochrome. Hence a chromogen, which is transformed by the enzyme to a visible signal (stain) needs to be added afterwards. This method leads to a more stable and even more sensitive results than with fluorochromes. Compared to the direct method, the indirect method is more sensitive and further a greater variety of primary antibodies are available. As with the direct method, some control slides should be included in each run. The enzymes, the chromogens, the primary antibody should be left out in a slide each. Again, one for sure positive and one negative slide is of importance. Other methods, such as the three-step-method, ABC-method, polymere-method, etc. are available but rarely used (52).

At the end of the procedure, counterstaining is performed. A colour high in contrast to the immunohistochemical stain is used to highlight the nuclei of the cells (52, 54).

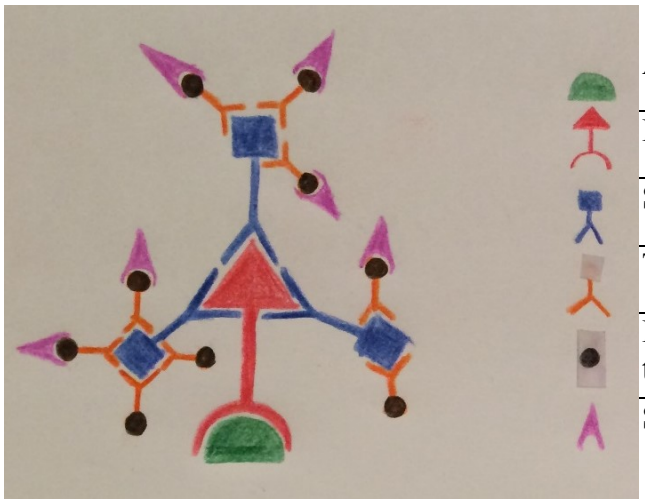

Antigen – BRAF V600E Mutation
Primary Antibody (murine) - monoclonal
Secondary Antibody – polyclonal
Tertiary Antibody – polyclonal
Horseradish peroxidase (HRP) – attached to tertiary AB
Staining

Figure 3 Antigen – Antibody Binding

IHC is nowadays not solely used for differentiating between positive and negative samples for a mutation, but can also count as a semi-quantitative assay, provided a standardized protocol is used. (57)

The following protocols were developed through trial and error. Modifying the different incubation times and temperatures, trying different chromogens and checking every single step has led to several versions:

For this project the antibody was first tested on BRAF V600E positive thyroid tissue with the chromogen Nova Red. The very first run was started off with an antibody concentration of 1:600 and an antibody incubation time of two hours. This first protocol lead to very unsatisfying results: very light stain which was mainly covered up by the counterstain. Therefore several experiments were started side by side, modifying different parameters (counterstaining, antibody concentration, antibody incubation time and incubation temperature). For the first run with skin tissue samples counterstaining was lightened up (from “Light” to “Very very light” mode), AB concentration was adjusted to 1:150 and the incubation time to overnight incubation (~12h) at an incubation temperature of 4°C. A run with 40 samples was carried out according to this protocol: Nova Red (Run 1).

BRAF V600E Immunohistochemistry Protocol – Nova Red (Run 1)

1. Dewax paraffin slides using the Leica XL autostainer (Leica CV5030 Workstation, Leica Biosystems, Nussloch, Germany)
2. Antigen retrieval: in decloaking chamber at 105°C for 15min in an EDTA pH 9 buffer (Novocastra™ Epitope Retrieval Solutions RE7119, Leica Biosystems) and leave to cool down to RT
3. Put the slides in slide chambers
4. Wash 3x with TBS
5. H_2O_2 (5% in TBS) for 5 min
6. Wash 3x with TBS
7. Put the slides in humidifying chamber
8. Block for 15 min at RT with SNIPER protein block (MACH 1 Universal HRP-Polymer Detection, Biocare, Concord, CA)
9. Incubate with primary antibody (Mouse Anti-BRAF V600E Antibody, clone VE1, 0,5 mL concentrate, REF: E19292,Spring Bioscience, Pleasanton, CA) **1:150** diluted with SNIPER antibody diluents (MACH 1 Universal HRP-Polymer Detection, Biocare, Concord, CA) overnight at **4°C**
10. Put the slides in slide chambers
11. Wash 3x with TBS
12. Incubate with MACH 1 probe (MACH 1 Universal HRP-Polymer Detection, Biocare, Concord, CA) for **15 min**
13. Wash 3x with TBS
14. Incubate with MACH 1 polymer (MACH 1 Universal HRP-Polymer Detection, Biocare, Concord, CA) for **30 min**
15. Wash 3x with TBS
16. Put the slides in humidifying chamber
17. Incubate with Nova red (Nova Red™ Chromogen Kit, Vector Laboratories, Burlingame, CA) for **8 min**, but keeping an eye on it
18. Wash 3x with TBS
19. Counterstain with Hematoxylin using the Leica XL autostainer (Leica CV5030 Workstation, Leica Biosystems, Nussloch, Germany) (use Very Very Light mode) and coverslip them

Later the protocol was again modified increasing the AB concentration to 1:100 and incubation overnight at room temperature (RT) in order to produce stronger staining results. A run of 40 slides was carried out with this protocol: Nova Red (Run 2).

BRAF V600E Immunohistochemistry Protocol – Nova Red (Run 2)

1. Dewax paraffin slides using the Leica XL autostainer (Leica CV5030 Workstation, Leica Biosystems, Nussloch, Germany)
2. Antigen retrieval: in decloaking chamber at 105°C for 15 min in an EDTA pH 9 buffer (Novocastra™ Epitope Retrieval Solutions RE7119, Leica Biosystems) and leave to cool down to RT
3. Put the slides in slide chambers
4. Wash 3x with TBS
5. H2O2 (3% in TBS) for 5 min
6. Wash 3x with TBS
7. Put the slides in humidifying chamber
8. Block for 30 min at RT with SNIPER protein block (MACH 1 Universal HRP-Polymer Detection, Biocare, Concord, CA)
9. Incubate with primary antibody (Mouse Anti-BRAF V600E Antibody, clone VE1, 0,5 mL concentrate, REF: E19292,Spring Bioscience, Pleasanton, CA) **1:100** diluted with SNIPER antibody diluents (MACH 1 Universal HRP-Polymer Detection, Biocare, Concord, CA) overnight at **RT**
10. Put the slides in slide chambers
11. Wash 3x with TBS
12. Incubate with MACH 1 probe (MACH 1 Universal HRP-Polymer Detection, Biocare, Concord, CA) for **40 min**
13. Wash 3x with TBS
14. Incubate with MACH 1 polymer (MACH 1 Universal HRP-Polymer Detection, Biocare, Concord, CA) for **40 min**
15. Wash 3x with TBS
16. Put the slides in humidifying chamber
17. Incubate with Nova red (Nova Red™ Chromogen Kit, Vector Laboratories, Burlingame, CA)for **10 min**, but keeping an eye on it
18. Put it into distilled water

19. Counterstain with Hematoxylin using the Leica XL autostainer (Leica CV5030 Workstation, Leica Biosystems, Nussloch, Germany) (use Very Very Light mode) and coverslip them

At the same time it was realised, that even though the staining was optimised and appeared stronger and redder, it was still very difficult to distinguish between the brown colour of the melanin and the Nova Red stain. Especially the computer analysis software "Positive pixel count", which is described later on, could not distinguish between these two colours very well. Thus a stain with a completely different colour from the same company was tested called Vina Green. The following protocol was developed for the chromogen Vina Green:

BRAF V600E Immunohistochemistry Protocol – Vina Green

1. Dewax paraffin slides using the Leica XL autostainer (Leica CV5030 Workstation, Leica Biosystems, Nussloch, Germany)
2. Antigen retrieval: in decloaking chamber at 105°C for 15 min in an EDTA pH 9 buffer (Novocastra™ Epitope Retrieval Solutions RE7119, Leica Biosystems) and leave to cool down to RT
3. Put the slides in slide chambers
4. Wash 3x with TBS
5. H2O2 (5% in TBS) for 5 min
6. Wash 3x with TBS
7. Put the slides in humidifying chamber
8. Block for 20 min at RT with SNIPER protein block (MACH 1 Universal HRP-Polymer Detection, Biocare, Concord, CA)
9. Incubate with primary antibody (Mouse Anti-BRAF V600E Antibody, clone VE1, 0,5 mL concentrate, REF: E19292,Spring Bioscience, Pleasanton, CA) 1:100 diluted with SNIPER antibody diluents (MACH 1 Universal HRP-Polymer Detection, Biocare, Concord, CA) overnight at 4°C
10. Put the slides in slide chambers
11. Wash 3x with TBS
12. Incubate with MACH 1 probe (MACH 1 Universal HRP-Polymer Detection, Biocare, Concord, CA) for 20 min
13. Wash 3x with TBS

14. Incubate with MACH 1 polymer (MACH 1 Universal HRP-Polymer Detection, Biocare, Concord, CA)for 30 min
15. Wash 3x with TBS
16. Put the slides in humidifying chamber
17. Incubate with Vina green (Vina Green™ Chromogen Kit, Vector Laboratories, Burlingame, CA) for 10 min, but keeping an eye on it
18. Wash in water
19. Counterstain with hematoxylin (2 x 30 sec wash with water, 5 sec hematoxylin, 2 x 30 sec wash with water, 2 x 30 sec wash with ethanol, 2 x 2 min wash with xylene) and coverslip them

Counterstaining protocol with Leica XL autostainer for Nova Red protocols:

1. Water (2 min)
2. Haematoxylin (5 sec)
3. Water (3 min + 3 min in separate containers)
4. Ethanol 90% (1 min)
5. Ethanol 100% (1,5 min + 1 min + 1 min in separate containers)
6. Xylene (1,5 min + 1,5 min in separate containers)

In order to verify the results gained by the IHC method, Restriction Digest method was also carried out on 13 of the samples. This method will be described later on.

2.2 Aperio XT Light Microscope Scanning

Aperio ScanScope Imaging machines are bright field microscopes. 120 samples are loaded into a tray. The correct magnification then needs to be chosen (20x or 40x). Calibration then is to be carried out with a representative sample. Thereafter the ImageScope machine takes a snapshot of each slide. The user needs to annotate the area of the slide to be scanned and determine so called “focus points”. The slides are picked up by a robotic arm, put on a tray and are moved back and forth through the “microscope field”. While moving through this field, a camera takes images leading to a resolution of 0,50 µm/pixel when choosing 20x and 0,25 µm/pixel when choosing a 40x magnification. The images are available in TIFF, CWS and JP2 formats. Once the image is on the screen, it can be magnified, annotated, analysed, etc. (58).

2.3 Visual Evaluation

After the images were made with the Aperio XT light microscope they were then evaluated by eye. Each slide was assigned a number from 0 to 3 depending on how strong the staining was (0- negative, 1- questionable positive, 2- weak positive, 3- strong positive). This has proven to be quite effective in other studies (19).The staining pattern of the BRAF V600E mutation is homogeneously throughout the cytoplasm and the whole tumour. The nuclei are not stained. (19, 59).

If the background was too strong to determine whether the sample was positive or not, the sample was excluded. Sometimes it is difficult to differentiate between melanin and the staining, especially in the case of Nova Red stain. If this was the case, the sample was excluded too.

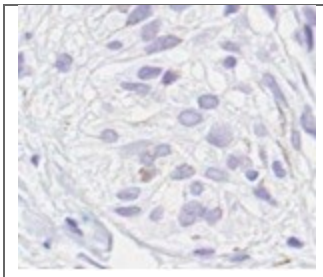	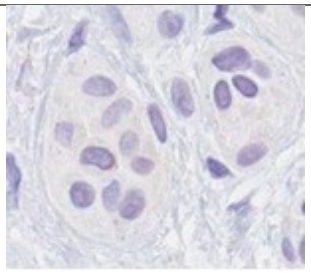	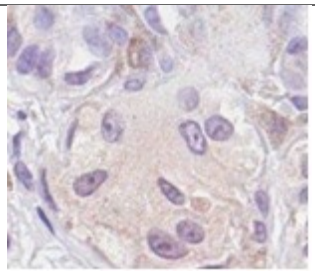	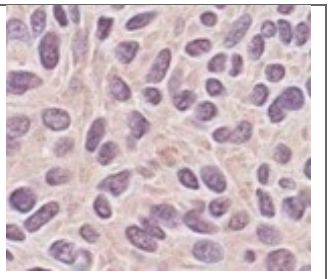
Nova Red – 0	Nova Red – 1	Nova Red – 2	Nova Red - 3
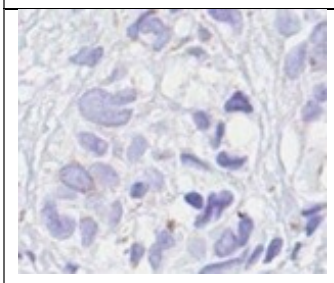	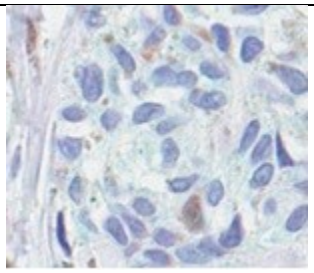	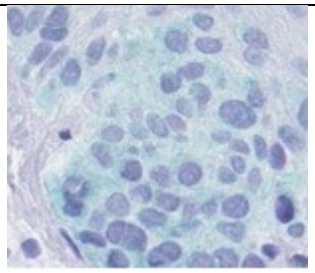	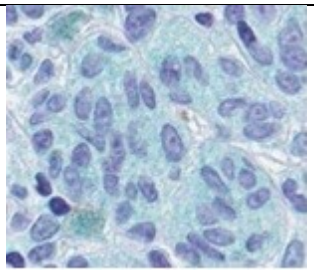
Vina Green – 0	Vina Green – 1	Vina Green – 2	Vina Green - 3

Table 5 Visual Evaluation – Sample Evaluation

2.4 Computer-aided Evaluation – Aperio ImageScope

The company producing Aperio XT ScanScope instruments also provides a free image software with analysis function called ImageScope. Several different algorithms are available among which the "Positive Pixel Count" can be found, a free version of the "Color Deconvolution Algorithm" produced by the same company. The positive pixel count detects and counts those pixels of an image (or defined area of an image) which is determined by the user by the means of three characteristics: Hue, Saturation and Intensity (4).

The colour chosen is called the "Hue". All the existing colours are represented by the rim of the circle. This hue is chosen by picking a spot on the rim of the circle. Each hue has a numeric value between 0,0 and 1,0, where Red = 0,0, Green = 0,33 and Blue = 0,66. All other colours can be found in-between. These parameters for defining a specific colour can be visualised by a colour wheel, as shown in Figure 4 (4).

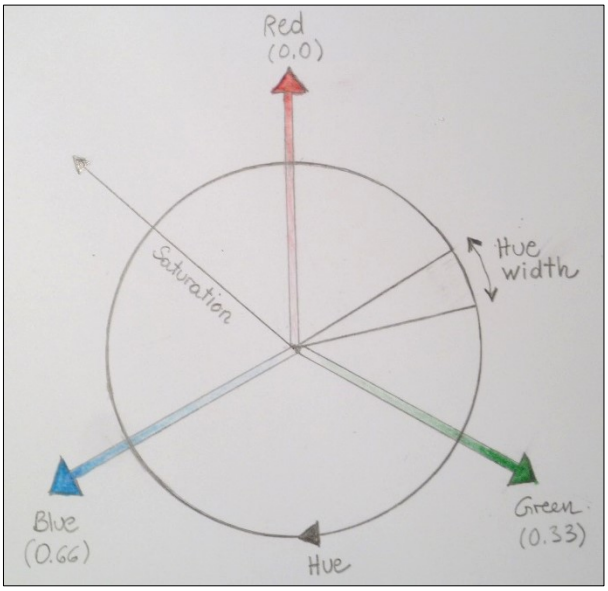

Figure 4 Colour Circle – Redrawn and Adapted from (4)

Saturation can be visualised by the purity of a colour. Full saturation (e.g. red) is situated on the rim of the circle whereas less saturated colours (e.g. pink) lie on the same vector as red but further to the centre of the circle, as shown in Figure 4 (4).

Hue width represents the portion of the circle included in the results, thus the amount of hues spread around the actual hue value. The smaller the hue width, the more precise the result specific to one colour. It can be seen as a "hue threshold value" (4).

Additional to these three criteria mentioned above, the "Intensity" and the "Density" can help filter out the desired colour. Intensity is the amount of light being able to transmit through the tissue. Thus the brighter a pixel, the higher its intensity. The algorithm assigns

the value 0 to black and 255 to bright white. Density on the other hand is defined as the light being blocked by the specimen (4).

To run an analysis with the positive pixel count algorithm, the following steps need to be followed:

1. Open the program ImageScope and retrieve an image.
2. Choose the free-hand pen or the rectangle tool to annotate an area to be analysed. A negative free hand pen can be used to exclude certain areas.
3. On the menu bar of ImageScope, click on "View". On the drop down, choose "Analysis". Select a macro (algorithm), which needs to be designed beforehand.
4. In order to fine-tune the macro, choose the button "Test".
5. In the window the following parameters can be modified (4):

View Width	Width of processing box
View Value	Height of processing box
Overlap size	Size of the overlap region for each view
Image Zoom	1,0 recommended for processing of all pixels
Markup Compression Type	Format of image
Compression Quality	Between 0 and 95
Classifier Definition List	Only applicable if used in conjunction with Genie
Class List	Only applicable if used in conjunction with Genie
Hue Value	Position on the colour circle
Hue Width	Colours clustered around the Hue width
Colour Saturation Threshold	Colours are represented with a grey component. A value between 0,0 and 1,0 can be chosen dependent on no grey or all grey component included respectively
Iwp (High)	Upper limit of intensity for weak positive pixels
Iwp (Low) = Ip (High)	Lower limit of intensity for weak positive pixels, upper limit of intensity for positive pixels
Ip (Low)= Isp (High)	Lower limit of intensity for positive pixels, upper limit of intensity for strong positive pixels
Isp (Low)	Lower limit of intensity for strong positive pixels
Inp (High)	Average of the red, green and blue component

Table 6 Positive Pixel Count – Input – Adapted from (4)

6. When modification is finished, click on "Run". The macro will be applied to the areas chosen and a result window will show the following results. These can then be saved in an Excel file.

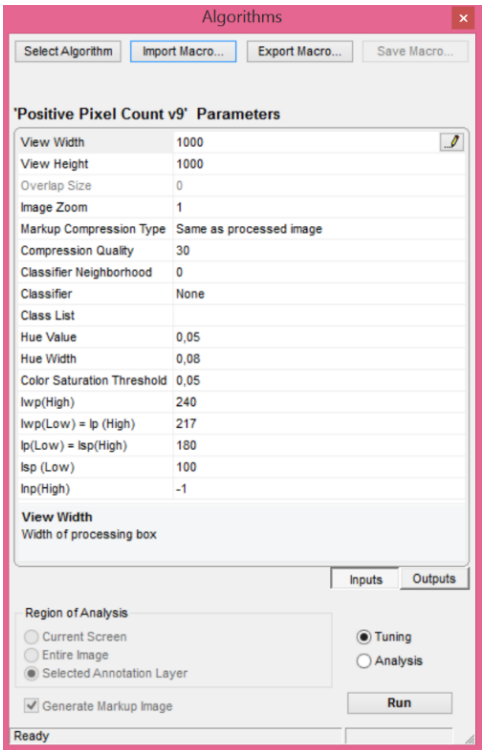

Figure 5 Positive Pixel Count – Screen Shot: Macro for Nova Red Stain (4)

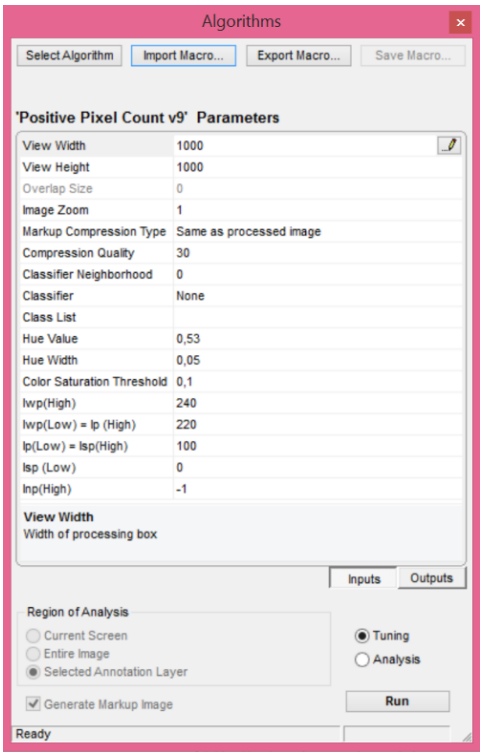

Figure 6 Positive Pixel Count – Screen Shot: Macro for Vina Green Stain (4)

The idea of this project was to count all BRAF V600E mutated positively stained cells by letting the program count the pixels with a specific colour. For this project, the samples were first assessed by eye. Once all of the input-values have been determined through trial and error, the slides were annotated: Three squares (50 x 50 µm) were drawn in the tumour tissue of each sample and evaluated by the "Positive Pixel Count Program" using the above macros (4). Then analysis was started.

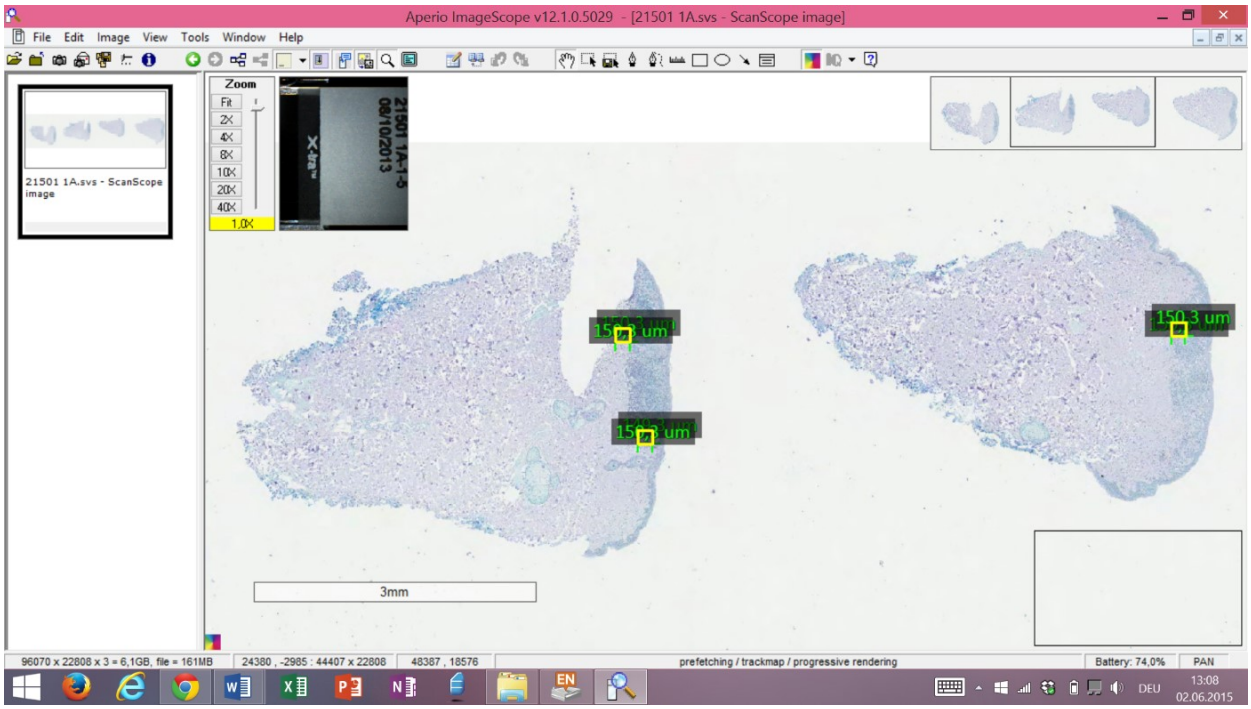

Figure 7 Screenshot of an Annotated Slide (3 squares of 50 x 50 µm) in the Aperio ImageScope Program

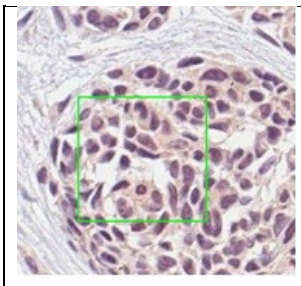 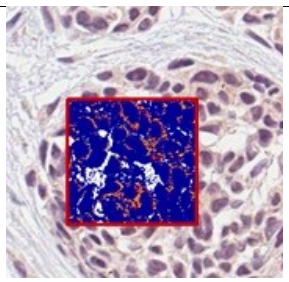	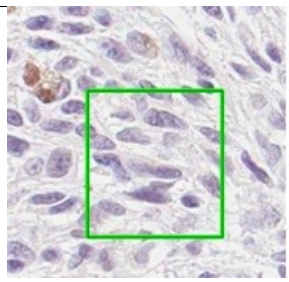 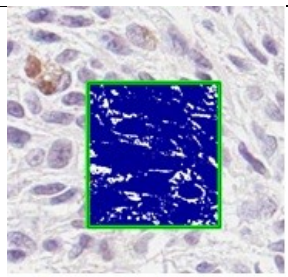
Nova Red-positive	Nova Red-negative
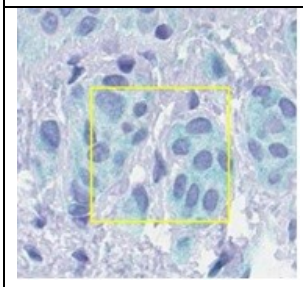 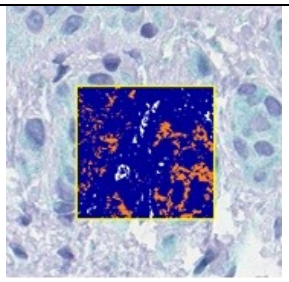	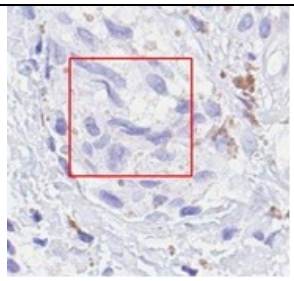 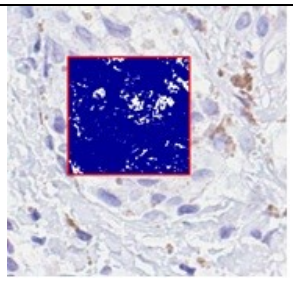
Vina Green-positive	Vina Green-negative

Table 7 Computer-aided Evaluation – Sample Evaluation

2.5 Genetic Verification of IHC Results with a Restriction Digest Method

To verify the visual and computer aided evaluation, the restriction digest method was applied to 13 of the samples.

2.5.1 DNA Extraction from FFPE Tissue Samples

This method was carried out with a kit from Macherey-Nagel called "DNA isolation from FFPE samples".

Instead of the usual 4µm thick paraffin cuts required for IHC, two 20µm thick cuts of each paraffin block were requested for this method. The tumour-containing tissue was scratched off the slide with a scalpel blade and collected in a test tube. Then the protocol was carried out according to the Macherey-Nagel kit (DNA isolation from FFPE samples, Macherey-Nagel, Düren, Germany). The protocol is cited from the instruction manual of the kit (60):

1. "Deparaffinize sample

   Add 400 µL Paraffin Dissolver to the sample.

   Incubate 3 min at 60°C (to melt the paraffin). Vortex the sample immediately (at 60°C) to dissolve the paraffin. Cool down sample to room temperature."

2. "Lyse sample

   Add 100 µL of "Buffer FL". Vortex vigorously.

   Centrifuge at 11,000 x g for 1 min. Two phases will be formed: a lower (aqueous) phase and an upper (organic) phase. Tissue material will be transferred to the lower (aqueous) phase. …

   Pipette 10 µL of Proteinase K solution directly into the lower (aqueous) phase. Mix the aqueous phase by pipetting up and down several times. …

   Incubate at room temperature for three hours to lyse sample tissue. …

   Vortex 5 s. Set heating block to 90°C."

3. "Decrosslink

   Add 100 µL of the Decrosslink Buffer D-Link to the tube and vortex gently to mix Buffer D-Link into the aqueous (lower) phase.

   Centrifuge at 11,000 x g for 30 seconds to obtain phase formation.

   Incubate at 90°C for exactly 30 minutes.

   Vortex 5 s and let cool down to room temperature (approx. 2 min)."

4. “Adjust binding conditions

   Add 200 µL ethanol (96-100%) to the tube and mix by vortexing (2 x 5 s).

   Spin down briefly (approx. 1 s at 1,000 x g) to achieve complete phase separation.”

5. “Bind DNA

   For each preparation, take one NucleoSpin® DNA FFPE XS Column (green ring) placed in a CollectionTube (2 mL).

   Pipette aqueous (lower) phase completely into NucleoSpin® DNA FFPE XS Column.

   Centrifuge for 30 s at 2,000 x g.”

6. “Wash and dry silica membrane

   1st wash: Add 400 µL Buffer B5 to the NucleoSpin® DNA FFPE XS Column. Centrifuge 30 s at 11,000 x. g. Discard Collection Tube with flow-through and place the column into a new Collection Tube (2 mL).

   2nd wash: Add 400 µL Buffer B5 to the NucleoSpin® DNA FFPE XS Column.

   Centrifuge for 2 min at 11,000 x g to dry the membrane. Discard the collection tube with flow-through and place the column into a new nuclease-free microcentrifuge tube.”

7. “Elute DNA

   Pipette 20 µL Buffer BE directly to the center of the silica membrane of the column. …

   Centrifuge for 30 s at 11,000 x g.”

8. Go into lower, aqueous phase with a pipette and take out the DNA mixture to use for further procedures described below.

   (52, 60)

2.5.2 Polymerase Chain Reaction (PCR)

The concept of PCR is based on a series of consecutive temperature changes. First, the DNA sample is mixed with buffer, primers, Taq-polymerase, dNTPs (Nucleoside triphosphate, which are precursors of nucleosides), betaine (enhancer solution) and water. This mixture passes through different steps:

Denaturation: The sample containing the double stranded DNA is heated to 94°C for a short time in order to split the double strand into two single ones.

Hybridisation: When cooled down to 45-60°C, primers, which are designed for a very specific region on the DNA strand, can bind to these single strands.

Extension: The mixture is then heated up again to 72°C, which is the optimum temperature for the Taq-Polymerase. The polymerase attaches the dNTPs to the specific gene-sequence of the single strands to produce a complementary strand.

These three steps are repeated around 30 times and the specific gene-sequence, which the primer is designed for, is therefore amplified exponentially (61).

First the amount of DNA of each sample needs to be determined, in order to add the correct amount of DNA to the PCR master mix. This was done with a spectrophotometer. If the DNA concentration was too high or low, it was compensated with the water in the master mix.

In this project the following substances were added per sample:

10 x TAE Buffer:	5 µL
Betaine:	10 µL
Primers:	1 µL forward Primer
	1 µL reverse Primer
dNTPs:	5 µL
Water:	23,75 µL
Taq-Polymerase:	0,25 µL
DNA	4 µL

The following temperature cycle was performed in this project:

94°C	-	12 min	→	1 x
94°C	-	45 sec	⎫	
56°C	-	90 sec	⎬	35 x
72°C	-	90 sec	⎭	
12°C	-	3 min	→	1 x

(61)

2.5.3 Restriction Digest Method

Restriction digest is a method to detect specific mutations and to test if this mutation is heterozygous or homozygous.

Primers are designed for a specific short sequence of nucleotides. In this case, the primer will only bind to the DNA, if the mutation is present. Thereafter the restriction enzyme (XbaI) binds and cuts the strand, leaving a longer (131 base pairs) and a shorter (27 base pairs) part of the strand behind. For the BRAF V600E mutation a primer binding to the following DNA sequence was designed by Mitchell Stark (62):

t a c a g t Wild type (no mutation)

t a c a g a V600E mutation (arrow shows restriction site)

After digestion with XbaI:

Wild type:	undigested	→	158 base pairs (very intense in gel electrophoresis)
Heterozygous:	one allele cut	→	158 base pairs (less intense in gel electrophoresis)
			131 base pairs
			27 base pairs (too small to see in gel electrophoresis)
Homozygous:	both alleles cut	→	131 base pairs
			27 base pairs (too small to see in gel electrophoresis)

The following protocol was used in this project for the Restriction Digest Method:

Substances per sample:

NEB #2 (Buffer for optimal enzyme activity):	3 µL
BSA 10x (bovine albumin serum – to prevent adhesion):	3 µL
Water:	9,75 µL
XbaI (Restriction Enzyme):	0,25 µL
PCR product:	20 µL

This mixture then needs to be incubated overnight (12 hours) at 37°C. Just before starting with the gel electrophoresis, it should be incubated at 65°C for 20 minutes in order to inactivate the enzymes (62).

2.5.4 Gel Electrophoresis

The concept of Gel Electrophoresis is based on the fact that nucleic acids are negatively charged and are therefore attracted to an anode. The separation of the DNA fragments depends on the voltage applied, the size of the pores of the gel and the size, charge and shape of the molecule (61).

For this project the following gel was prepared:

3% Agarose Gel: 150 mL TAE-Buffer

4,5 g Agarose

12 µL Ethidium Bromide

This mixture is heated in a microwave with intermediate stirring until the Agarose dissolved completely. It is then poured into a plate and a comb for producing wells is fixed. After cooling down and thickening, the plate is filled with TAE-buffer until the gel is just covered. A 100 base-pair ladder is pipetted into the first well. Next 8 µL of each DNA sample is pipetted into a well each. Finally two samples with a known homozygous BRAF V600E mutation, two samples with a heterozygous BRAF V600E mutation and two wild types are pipetted into separate wells. Finally voltage of 100V is applied and the separation is left to run for 1,5 hours (61, 62).

After the above procedure the gel is removed from the plate and inspected under UV light. With a camera, pictures of the gel with the illuminated bands can be taken.

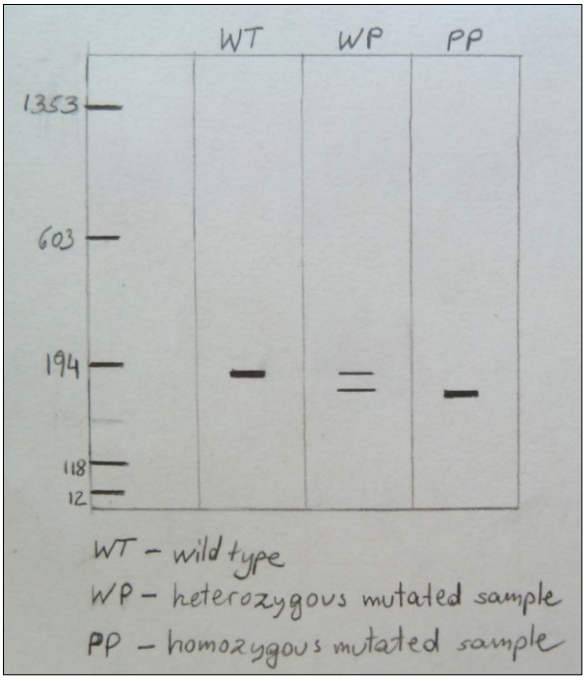

Figure 8 Restriction Digest – Gel Electrophoresis Interpretation

Wild type: single, intense band closer to the origin

Heterozygous for the BRAF V600E mutation: two bands

Homozygous for the BRAF V600E mutation: single, intense band closer to the terminal end

(62-64)

Figures 9 and 10 show the original gels of the experiment during inspection under UV light. Base pair "ladders" were pipetted on the outer lanes for reference. Except for the first lane, all the other numbered lanes contain test samples. "Ko" represents the three "control samples".

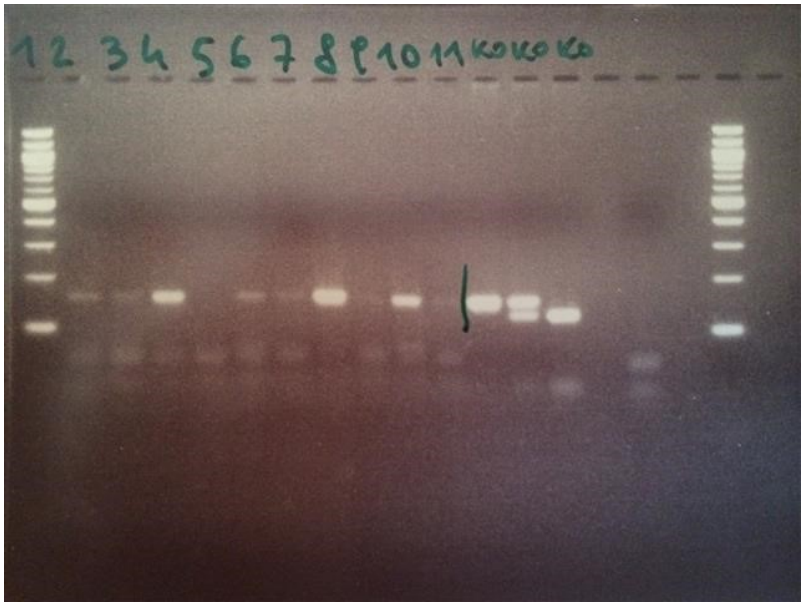

Figure 9 Gel Electrophoresis Plot (Lane 1= 100bp ladder, Lanes 2-11= test samples, Ko= control samples)

Figure 10 Gel Electrophoresis Plot (Lane 1= 100bp ladder, Lanes 2-6 = test samples Ko= control samples)

Due to the low quality of the DNA which was obtained from the paraffin samples, the interpretation of the results of the gel electrophoresis was difficult and in some cases not possible. Therefore the results obtained by the restriction digest method were not included in this diploma thesis.

2.6 Genetic Verification of IHC Results with a MassArray Platform

2.6.1 DNA Isolation

By looking at H&E stained tissue sections of the samples, tumour areas were determined. Punch biopsies (2 mm) were then extracted from formalin fixed and paraffin embedded tissue blocks from areas high in tumour tissue. The tissue extracted was then deparaffinised with xylene and washed two times in ethanol. Thereafter, DNA was extracted with an FFPE kit (Qiagen GeneRead DNA FFPE Kit, Germany). Additionally, the sample was exposed to another 3 hours of proteinase K digestion at 56°. For quantification of the DNA extracted a spectrophotometer (Life Technologies, Carlsbad CA) was used. Further the DNA quality was checked by using a 2% Agarose gel (Amresco, Solon, OH).

2.6.2 Genotyping

Genotyping was carried out with a MassArray platform. A multiplex assay testing for mutations on the following 20 genes was used (MelaCarta Panel, Agena Bioscience, San Diego, CA): KIT, KRAS, MEK. MET, NEK10, NRAS, PDGFRA, PIK3CA, PTK2B, RoR2, AKT3, BRAF, CDK4, CXCR4, CTNNB1, EPHA10, EPHB6, ERBB4, GNA11, GNAQ (65).

The data gained with the MelaCarta Panel were then confirmed and combined with the "Ultraseek Oncogene panel". This panel tests for mutations on the following genes: ALB1, AKT1, ALK, BRAF, EGFR, FLT, IDH1, IDH2, JAK2, KRAS, NRAS, PIK3CA (66).

The combined results of these two genotyping methods was used as the "gold standard" in this experiment. Thus all results were compared to these.

MassArray System

The detection starts off with a multiplex PCR. Thereafter a mutation-specific single base extension reaction follows, which applies a single mutation-specific chain terminator tagged with a moiety for solid phase capture. Subsequently washing and elution takes place and analysis is started with the MassArray System. This MassArray System consists of a SpectroCHIP and MALDI-TOF method (66).

3 Results

There were 73 different malignant melanoma samples included in the study. Due to insufficient fixation of the tissue, too little tissue on the slide or very heavy background 11 of these samples were excluded. Of the 62 samples left, 18 samples (29%) were tested positive by genotyping, the gold standard.

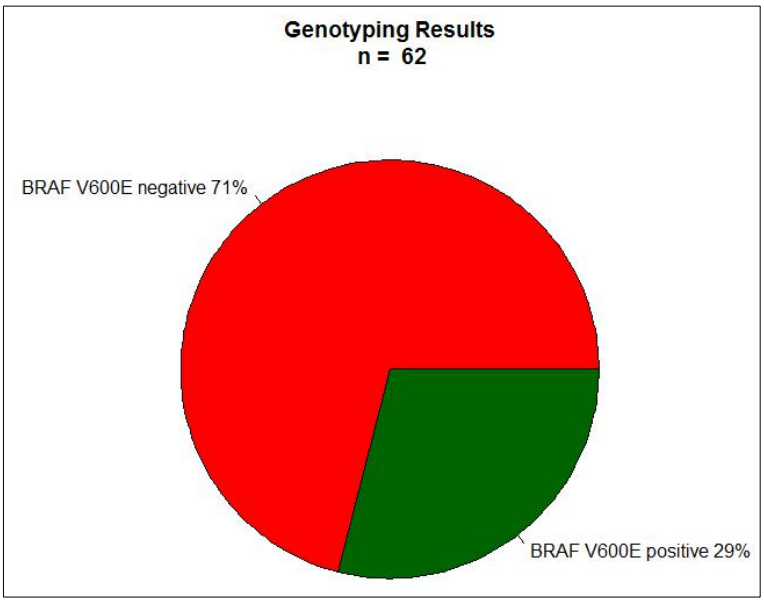

Figure 11 Genotyping Results

Visual evaluation of the 62 samples stained with Nova Red resulted in 36 negative (58%), 11 questionable positive (18%), 7 weak positive (11%), 8 strong positive (13%).

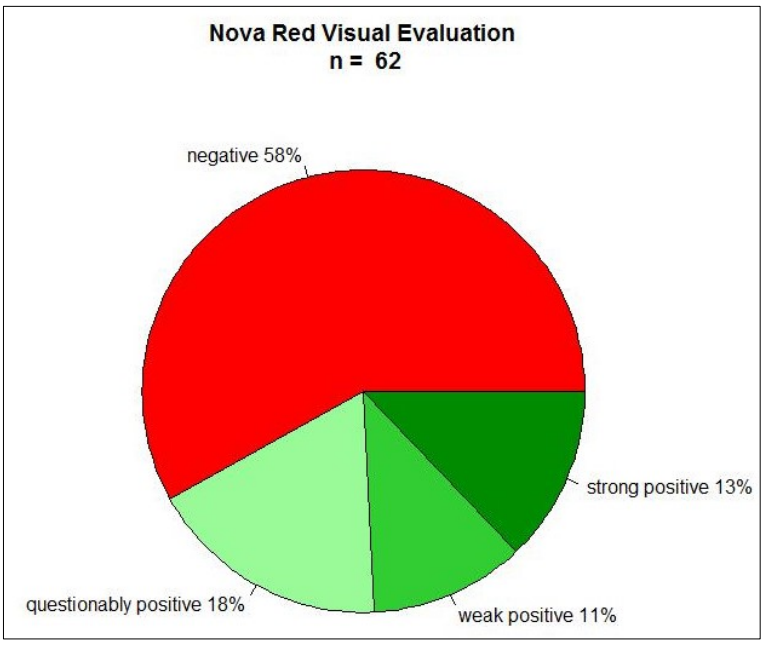

Figure 12 Nova Red Visual Evaluation

Of the 73 samples stained with Nova Red, 38 samples were also stained with Vina Green. 7 samples were excluded due to the same reasons as above or because they were excluded from the Nova Red experiment. Visual evaluation of these 31 samples resulted in 20 negative (65%), 9 questionable positive (29%), 1 weak positive (3%) and 1 strong positive (3%).

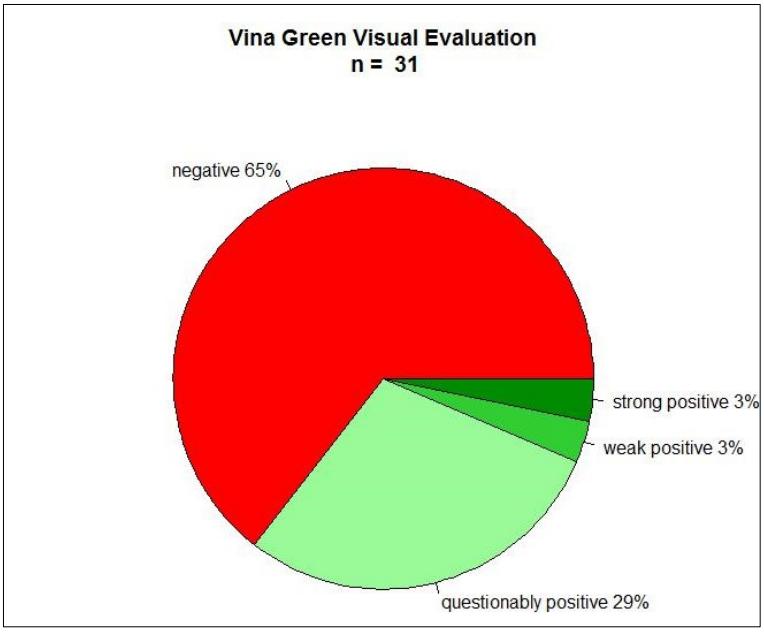

Figure 13 Vina Green Visual Evaluation

According to literature and in order to simplify the statistical analysis, the negative and the questionable positive samples are summarized to "visually negative" samples. The weak positive and the strong positive samples are on the other hand summarized to "visually positive" samples (67).

As represented in Figure 14, 41 of the visually negative evaluated samples stained with Nova Red showed a negative result in the genotyping as well. Of the 15 visually positive evaluated samples, 12 are in accordance with a positive genotyping result. Thus 3 samples were false positive compared with the genotyping result (genotypically negative but visually positive). 6 false negatives (genotypically positive but visually negative) were recorded. Thus the specificity ($\frac{true\ negative}{true\ negative+false\ positive}$) is 93,1%; the sensitivity ($\frac{true\ positive}{true\ positive+false\ negative}$) is 66,7%. 85,5% show coherent results in IHC and genotyping ($\frac{true\ positive+true\ negative}{number\ of\ all\ samples\ tested}$).

Figure 15 shows that 53 of the 62 samples are in accordance when comparing the results of the genotyping and the visual evaluation method, thus show negative or positive results in both. 9 of the visually evaluated samples are either false positive or false negative compared to the genotyping results. Therefore the concordance is substantial with a Cohen's Kappa of 0,63 (95% CI, 0,41 to 0,85) and a p-value of 0,000000589.

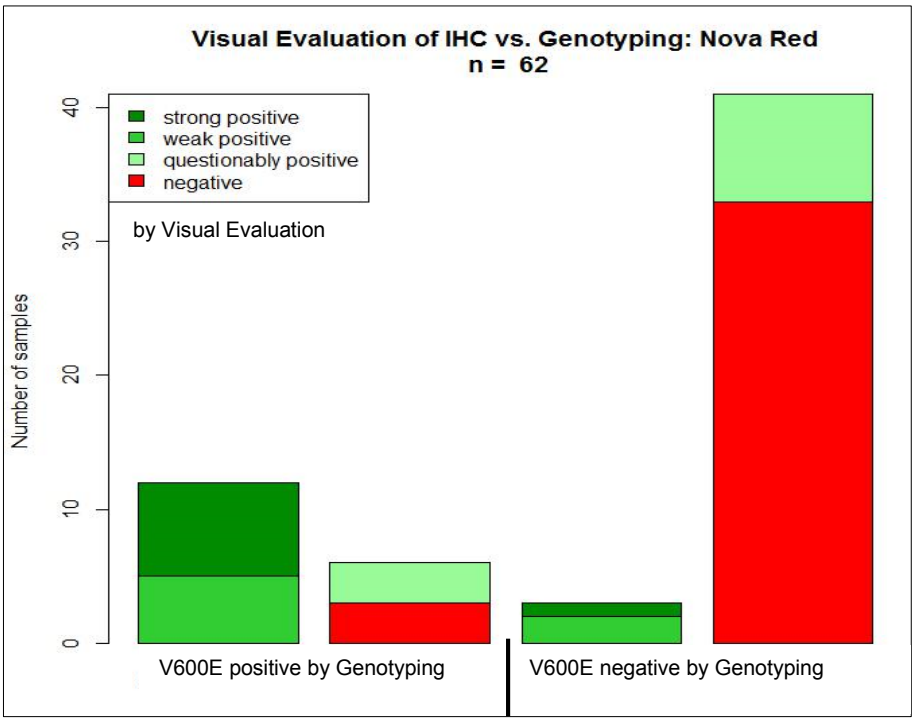

Figure 14 Visual Evaluation of IHC vs. Genotyping: Nova Red

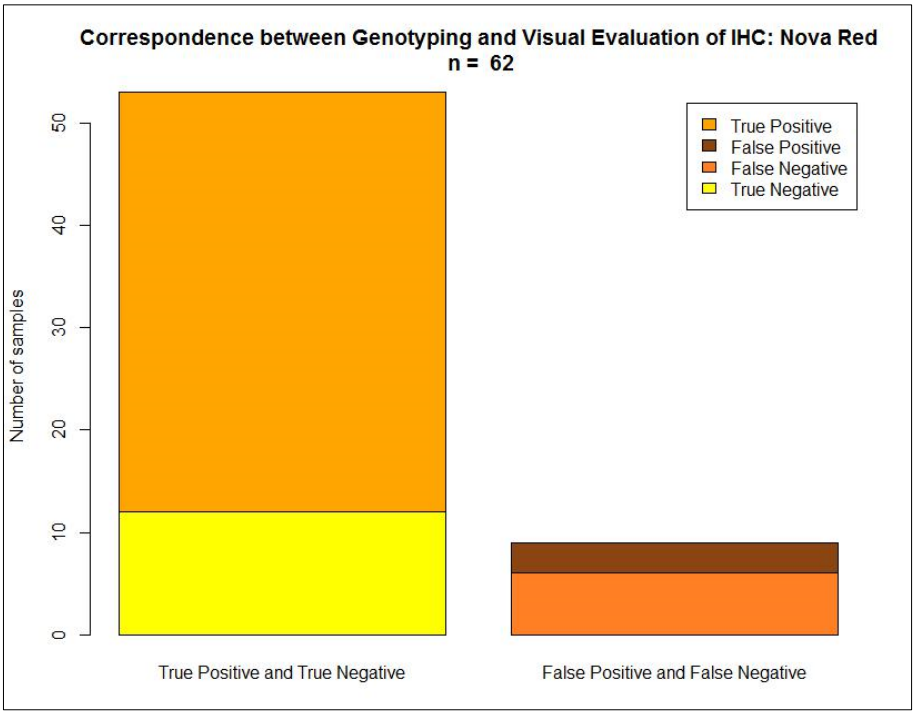

Figure 15 Correspondence between Genotyping and Visual Evaluation of IHC: Nova Red (Specificity: 93,1%, Sensitivity: 66,7%)

As seen in Figure 16, only 2 samples were visually evaluated positive when stained with Vina Green, but 6 samples were found to be positive when evaluated with genotyping. Thus 4 samples are false negative by visual evaluation. No false positive samples were found. The sensitivity for IHC with Vina Green is therefore 100%, but the specificity is only 33,3%. 87,1% of the samples deliver coherent results in both IHC and genotyping (gold standard).

Figure 17 shows that 27 of the 31 samples are in accordance when comparing the results of the genotyping and the visual evaluation method, thus show negative or positive results in both. Therefore the concordance is moderate with a Cohen's Kappa of 0,45 (95% CI, 0,02 to 0,87) and a p-value 0,00284.

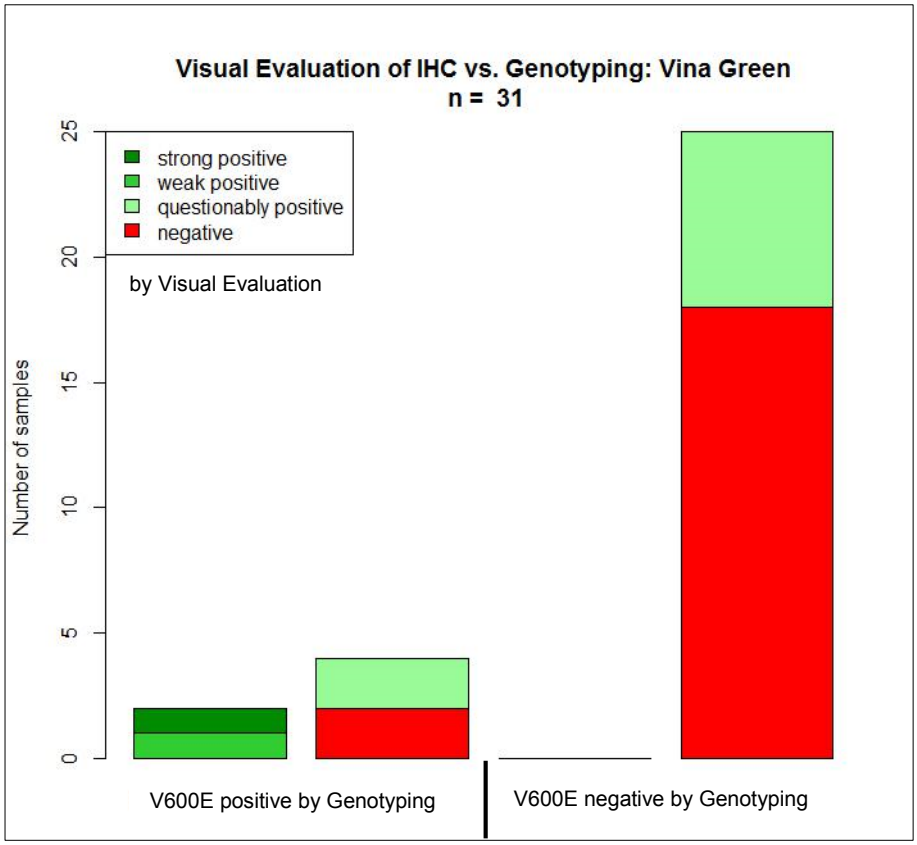

Figure 16 Visual Evaluation of IHC vs. Genotyping: Vina Green

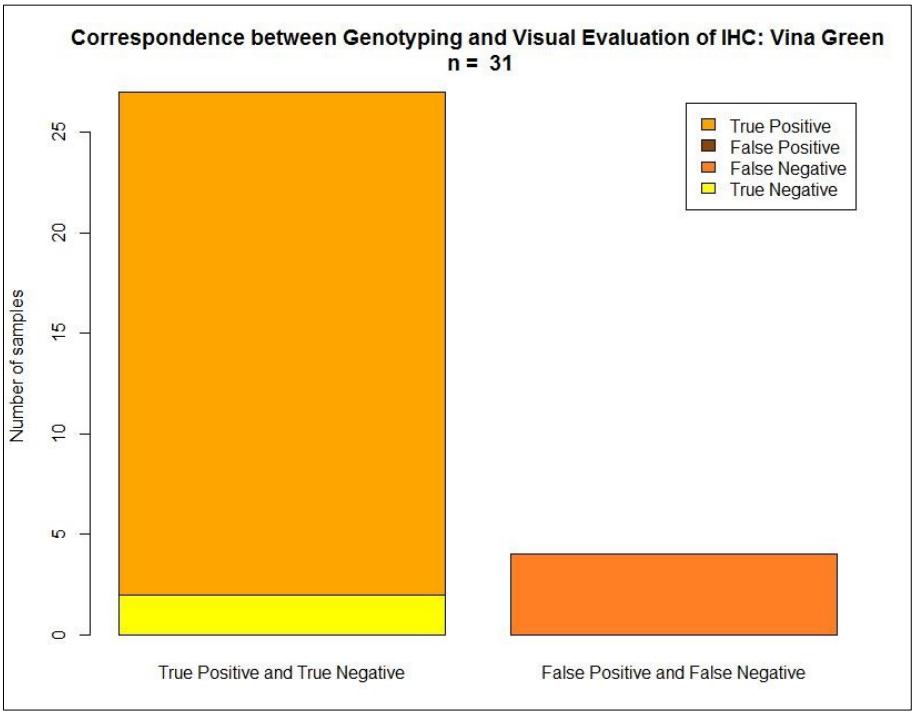

Figure 17 Correspondence between Genotyping and Visual Evaluation of IHC: Vina Green (Specificity: 33,3%, Sensitivity: 100%)

As can be seen in Figure 18, 84% (26 samples) of the samples stained with Nova Red and Vina Green are negative in both. 6% (2 samples) were found to be positive in both. 10% (3 samples) showed no accordance (negative in one and positive in the other or vice versa). 90,3% of the samples deliver coherent results with Nova Red and Vina Green.

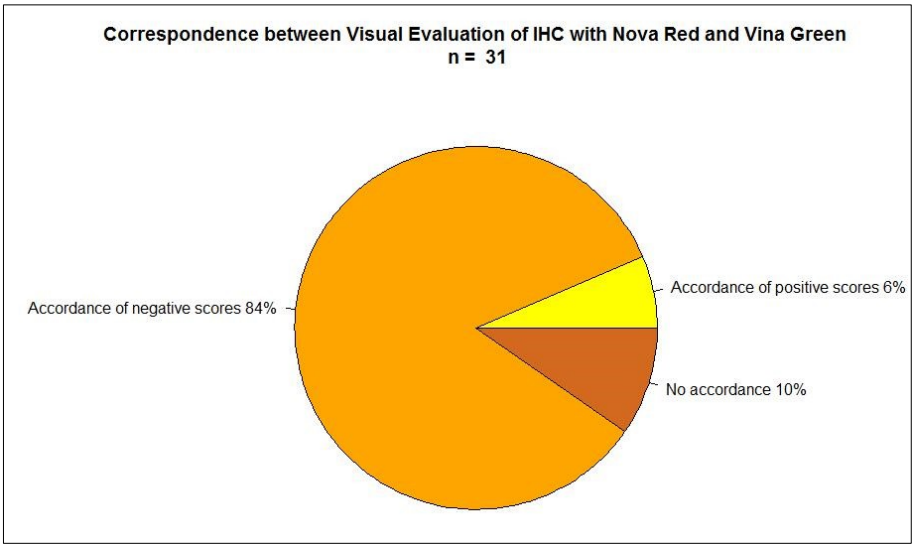

Figure 18 Correspondence between Visual Evaluation of IHC with Nova Red and Vina Green

The concordance of the results of IHC carried out with Nova Red and Vina Green is moderate with a Cohen's Kappa of 0,53 (95% CI, 0,08 to 0,98) and a p-value of 0,000855.

A clear difference in positivity-values (percentage of positive pixels per total area analysed in a sample) of the Nova Red samples assessed with the help of a computer evaluation program cannot be detected between the genotypically evaluated positive and negative samples. The median positivity-value of the genotypically positive samples is 10,59%, of the negative samples 0,86%. The negative samples are clustered around the median (Q1=0,14%, Q3=4,49%), whereas the positive samples show a greater spread (Q1=1,17%, Q3=18,02%). There is quite a broad field where the first quartile of the staining positivity of the genotypically positive and the third quartile of the genotypically negative overlap (1,17-4,49%). Due to the overlap the computer-aided evaluation cannot ensure that samples with staining positivity between 1,17 and 4,49% are correctly evaluated as positive or negative.

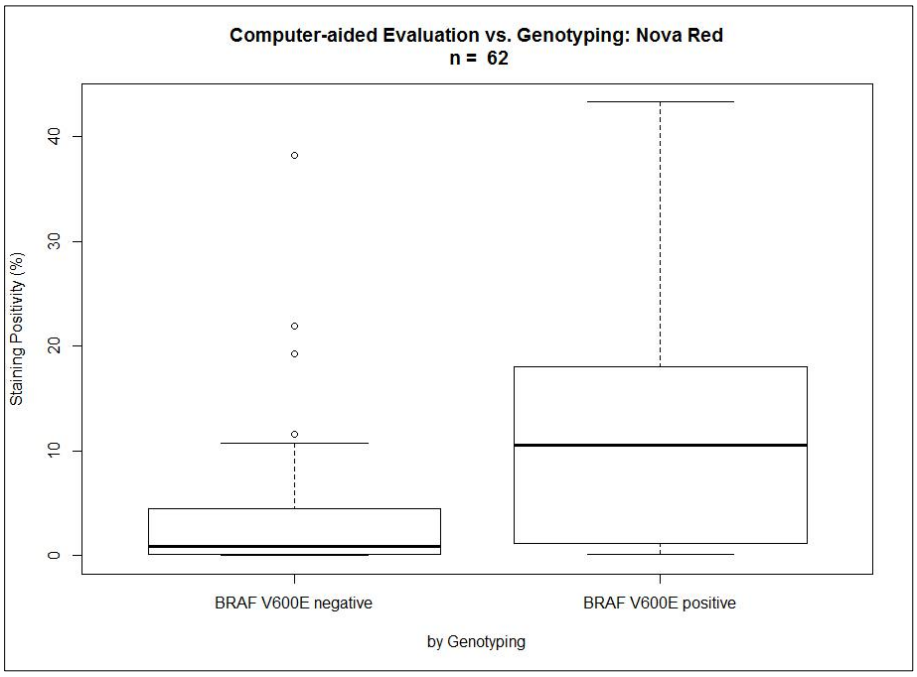

Figure 19 Computer-aided Evaluation vs. Genotyping: Nova Red

A clear difference in positivity-values of the Vina Green samples assessed with the help of a computer evaluation program cannot be detected between the genotypically evaluated positive and negative samples. The median value of the positive samples is 0,13%, of the negative samples 0,04%. The negative samples are clustered around the median (Q1=0,02%, Q3=0,32%), whereas the positive samples show a large spread (Q=0,02%, Q3=7,23%). The first quartile of the genotypically positive and the third quartile of the genotypically negative overlap completely. Due to the overlap the computer-aided evaluation cannot ensure that samples with staining positivity are correctly evaluated as positive or negative.

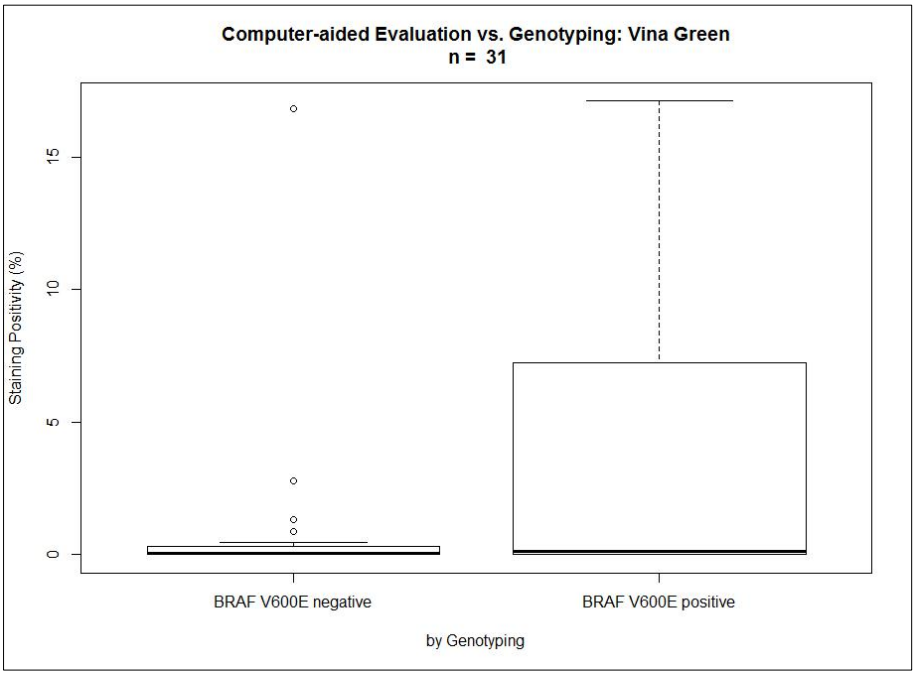

Figure 20 Computer-aided Evaluation vs. Genotyping: Vina Green

As shown in Figure 21 no correspondence of the staining positivity between Nova Red and Vina Green can be detected, as no visible pattern or structure can be found. Neither dependence nor independence could be found.

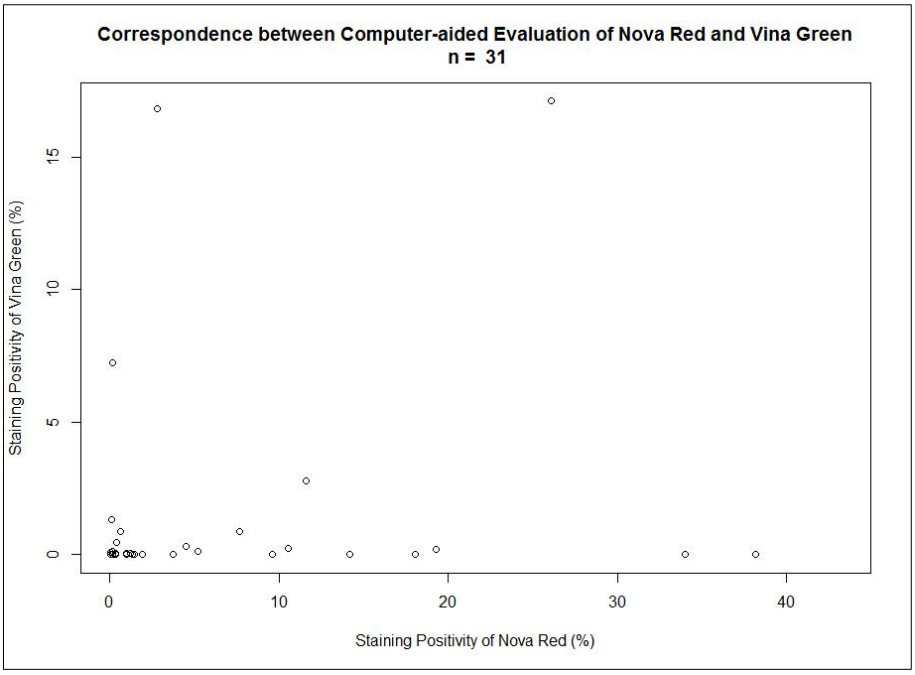

Figure 21 Correspondence between Computer-aided Evaluation with Nova Red and Vina Green

Figure 22 depicts the association between computer-aided and visual evaluation in samples stained with Nova Red. The visually negative samples also show the lowest median of the staining positivity values (0,57%) in the computer-aided evaluation and the visually strong positive samples show the highest median of the staining positivity values (10,72%). The questionable and the weak positive samples have median staining positivity values of 7,66% and 2,12% respectively.

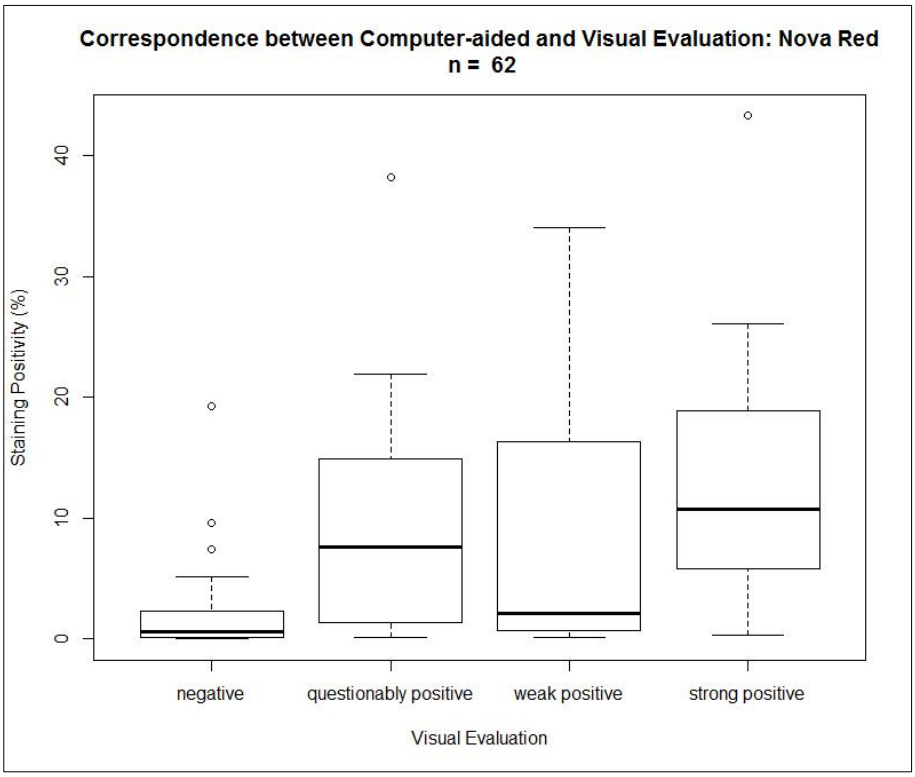

Figure 22 Correspondence between Computer-aided and Visual Evaluation: Nova Red

Figure 23 shows that the median staining positivities of the computer aided evaluation of the IHC with Vina Green correspond to the categories of the visual evaluation. The staining positivities are 0,02%, 0,88%, 7,23% and 17,12% for negative, questionable positive, weak positive and strong positive visual evaluation respectively. Thus the visual and the PC-aided evaluation correspond greatly.

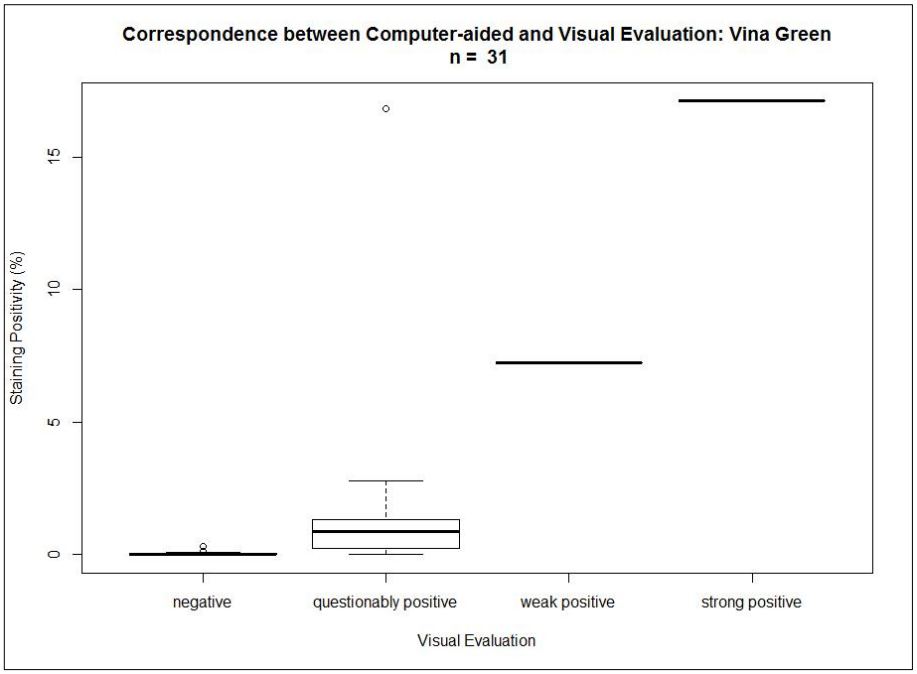

Figure 23 Correspondence between Computer-aided and Visual Evaluation: Vina Green

Finally, models were considered in order to predict the probability of actually being BRAF V600E positive based on the results of the IHC staining method. Unfortunately, models using VinaGreen did not seem to be statistically significant.

First, a Logit model for the visual evaluation of the IHC with Nova Red was established. It shows, that the probability for being genotypically positive is 77 times as high if rated "strong positive" when compared to a sample being rated as "negative". Being "weak positive", the probability for the sample being genotypically positive is 27,5 times higher than when rated "negative". The probability of a sample being "questionable positive" on the other hand is only 4,13 times as high for being genotypically positive compared to negative samples.

A Logit-model can also be set up for the computer-aided evaluation of IHC with Nova Red as predictor and genotyping as response. The probability of being genotypically "BRAF V600E positive" is estimated as follows:

$$P(\text{Genotyping} = \text{"BRAF V600E positive"}) = \frac{e^{\hat{\beta}_0+\hat{\beta}_1*\text{Positivity}}}{1+e^{\hat{\beta}_0+\hat{\beta}_1*\text{Positivity}}} \approx \frac{e^{-1.44032+0.08093*\text{Positivity}}}{1+e^{-1.44032+0.08093*\text{Positivity}}}$$

Hence, the probability for instance for a positivity of 50% in the computer-aided evaluation of IHC which is 0,931 can easily be predicted. For a positivity of 10% it is 0,347 and for 0,1% positivity the estimated probability is still 0,192.

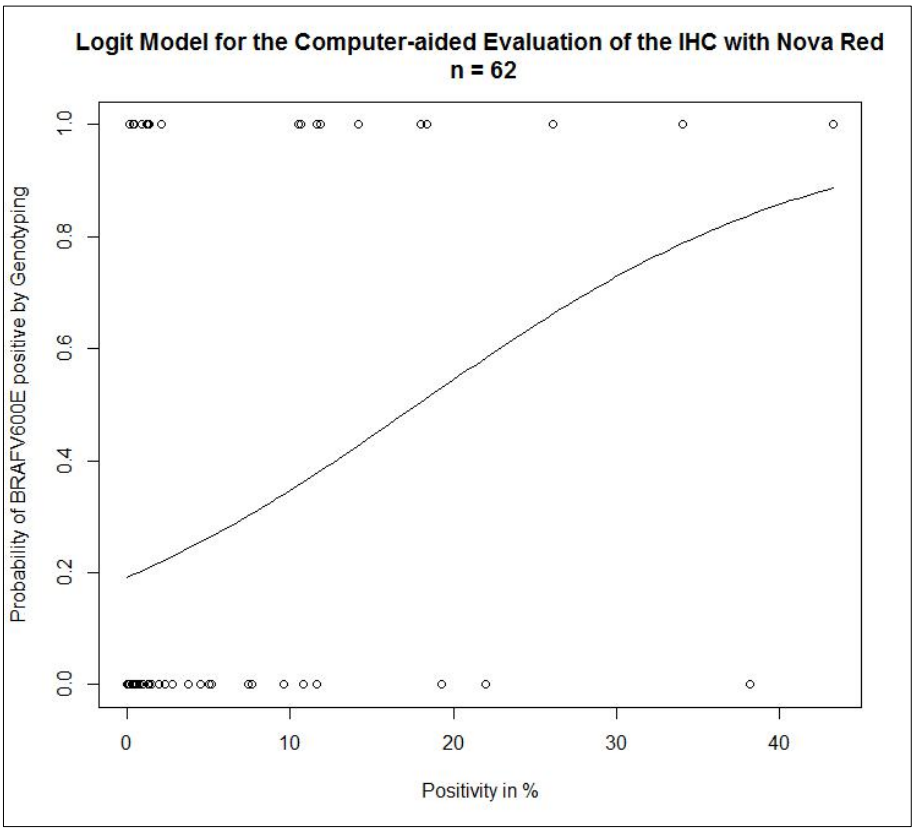

Figure 24 Logit Model for the Computer-aided Evaluation of the IHC with Nova Red

Summary of Results:

		Nova Red	Vina Green
IHC Visual Evaluation	Sensitivity	66,7%	100%
	Specificity	93,1%	33,3%
	Coherent with Genotyping	85,5%	87,1%
	Cohen's Kappa	0,63 (95% CI, 0,41 to 0,85), p=0,000000589	0,45 (95% CI, 0,02 to 0,87), p=0,00284
IHC Computer-aided Evaluation	Median positive value	10,59%	0,13%
	Q1 of the positive value	1,71%	0,02%
	Q3 of the positive value	18,02%	7,23%
	Median negative value	0,86%	0,04%
	Q1 of the negative value	0,14%	0,02%
	Q3 of the negative value	4,49%	0,32%

Table 8 Summary of Results of Different Immunohistochemical Evaluation Methods

4 Discussion

Importance of Immunohistochemistry in Diagnostics of the BRAF V600E Mutation

According to Colomba et al., immunohistochemistry with the VE1 antibody is the most specific method for the detection of a BRAF V600E mutation compared with directional Sanger sequencing of PCR products, real-time PCR and pyrosequencing (68). Various studies show, that immunohistochemistry has also proven to be a reliable detection method, which is highly sensitive and specific (variable studies show a sensitivity and specificity of 90-100%) in other tumours (colorectal cancer, etc.) with the BRAF V600E mutation (69-71). False negatives have rarely been detected, but false positives are sometimes the case (71, 72). A different study comparing five different methods of BRAF V600E detection found that IHC "was a good amendment to HRM [high resolution melting analysis]" and only showed cross-reactivity once (59).

Genotyping by MALDI-TOF: Results Compared to Other Studies

When looking at the various methods to detect a BRAF V600E mutation in clinical settings, usually some form of genotyping is considered first. Different methods for testing this mutation with genotyping are available (Directional Sanger Sequencing of PCR products, Real-Time PCR, Pyrosequencing and High Resolution Melting Analysis, etc.) MassArray with MALDI-TOF as a detector has been established for SNP detection and has been used as the gold standard in this experiment. Various papers support the success of this method (73, 74).

According to Menzies et al., roughly 50% of all melanoma carry a mutation on the BRAF gene, of which 70-90% are positive for specific V600E mutation. Thus it was expected to find 35-45% of the samples tested to be positive for the BRAF V600E mutation (19). Genotypically 29% of the samples were found to be positive. The small number of positive samples found with genotyping could be due to the small number of samples in general (n=62).

Immunohistochemistry: Possible Flaws in the Method and the Visual Evaluation

Immunohistochemically, combining strong and weak positive results, 24% were visually evaluated as positive when stained with Nova Red, but only 6% when stained with Vina Green.

The specificity of the IHC with the chromogen Nova Red is 93,1% and the sensitivity is 66,7%. 85,5% of the samples show coherent results with genotyping. Comparing these results with other literature (Liu et al.: specificity: 100%, sensitivity: 72,2%, 93,8% coherent with genotyping results), our results are marginally poorer. The results of IHC with Vina Green are as follows: sensitivity: 100%, specificity: 33,3%. 87,1% show coherent results with genotyping.

The 3 false positive results in visual evaluation of the Nova Red experiment could be explained with a sampling error. Thus there might not have been used enough or suitable tumour tissue for genotyping leading to negative results with the genotyping method (MALDI-TOF) but positive results in the IHC experiment. Vina Green does not have any false positive results.

The fact that specificity, sensitivity and concordance are not as high as in literature can be lead back to different reasons. The IHC-staining in this experiment was carried out by hand. It was tried to keep all the incubation times constant and to treat each sample equally but it cannot be guaranteed that these parameters were kept exactly the same over the whole experiment. Most reference papers carried out the staining with an autostainer. This guarantees equal treatment and leads to stronger, more consistent and satisfactory staining which makes it easier for evaluation (72).

Further the background is the same for all samples when using an autostainer. Background caused the greatest problems for visual and computer-aided evaluation in this experiment. Often it was very difficult to differentiate between background and staining or between melanin and staining.

IHC is error-prone. Each step bears the possibility for an error, especially if carried out by hand. For example, using slide chambers speeds up the process of pipetting the different substances onto the slide but it cannot guaranteed that the whole tissue is covered with the substance and thus the staining may not be as successful. Further the “washing steps” may not be as efficient with the slide chambers. Therefore considerations need to be undertaken whether to place the slides side by side in a humidifying chamber in order to avoid slide chambers or to condone them. Avoiding slide chambers leads to a better staining quality but

the samples would need to be split up into several runs in order to spread out the slides side by side in a humidifying chamber. On the other hand, splitting up the samples into different runs leads to run-to-run discrepancies as the conditions might never be exactly the same.

Further the false negatives could result from tissue coagulation and early necrosis. Both factors lead to an impairment of antigenicity of the epitope (75).

Two types of monoclonal antibodies are available for the detection of the V600E mutation: the monoclonal VE1 and the anti-B-Raf. According to Routhier et al. the VE1 showed better results (97% concordance with genotyping) than the anti-B-Raf (88% concordance with genotyping), which is why the first one was chosen (55).

A study by Menzies et al. showed that the staining pattern of the BRAF V600E mutation is homogeneous throughout the cytoplasm and the whole tumour (19, 59). Thus as long as the tumour is included in the histological section, it should be possible to test for the mutation with IHC, independent of which part of the tumour is represented on the slide. Caution is still recommended, as also 80% of benign naevi display a V600E mutation on the BRAF gene (75). Therefore histopathological evaluation is very important before carrying out IHC, as a positive IHC result is also very likely in naevi.

Concerning background, visual evaluation of the IHC samples permits the investigator to "mentally subtract" the background to some extent and thus judge whether the tumour cells are stained stronger than the background or not. The computer algorithm cannot take the background into account at all and therefore a higher "staining positivity" does not necessarily imply a BRAF V600E mutation. With the exception of a few samples, the computer-aided and the visual evaluation still correspond quite well.

When assessing the tissue, we faced the same problems as described in other literature: differentiating between score 0 ("negative") and score 1("questionable positive") turned out to be particularly difficult and lead to most pathologist-to-pathologist scoring discrepancies. The ability to differentiate between background and true staining proved as very difficult as well. To solve this problem, Fisher et al. published a study about stringent immunohistochemistry scoring criteria for evaluating IHC stained melanoma with the monoclonal VE1 antibody. These guidelines lead to significantly better kappa scores and could therefore be used as an improvement to our study (37).

Immunohistochemistry: Clinical Applicability

When considering the applicability of immunohistochemical BRAF V600E detection with Nova Red to a clinical setting, the medication Vemurafenib would have been given to 15 patients, of which 3 patients would not have required it (if patients with a weak and strong positive result received medication). Six patients in need of the medication were not found with immunohistochemical methods. When looking at the Vina Green results, the medication Vemurafenib would have been withheld from 4 of the 6 patients requiring it. No false positive were found, thus no patient would have received the medication not requiring it. Thus immunohistochemical methods cannot be recommended for clinical application.

Computer-aided Evaluation of IHC

When looking at the results of the computer-aided evaluation, there is only a very small range of positivity-values (percentage of positive pixels per total area analysed in a sample), where medication is not recommended: 0,0 - 1,17%. Between positivity values of 1,17% and 4,49%, a verification of the result with a different method is recommended for sure, as neither a positive nor negative result can be ruled out. Any sample with a positivity value above 10,59% is very likely to carry a BRAF V600E mutation and could possibly be entitled to a therapy with Vemurafenib.

To improve the computer-aided evaluation, the positivity of the background could be measured on non-tumour containing tissue and then subtracted from the positivity measured in tumour cells. This on the other hand can turn out to be quite effortful and time-consuming. Simple evaluation by eye should be considered again as it may be more reliable. Furthermore, analysation programs, which can recognize certain cells or cell patterns (tumours), have been developed. Complementing the colour recognition with this cell pattern recognition feature could make the computer-aided evaluation a helpful tool in the future.

Genotyping by Restriction Digest

Several weaknesses in the method may have led to the low quality of the outcome of this experiment: Extracting DNA from two 4µm thick FFPE sections yields only very little DNA, especially if the sample is small. This may lead to a small DNA concentration in the PCR and gel electrophoresis which again results in only faint bands on the gel. These are then very difficult to assess.

When carrying out the PCR, pre- and post-PCR working steps were performed in different rooms to prevent contamination. Further control samples without DNA were included to check for contamination and prevent false-positives.

False negatives may be brought about by bad quality of the DNA or if PCR inhibiting substances (which are often present in paraffin sections) are in the mixture. The positive controls worked well in this experiment but the DNA concentration was very high for these compared to the other samples.

Interpretation of the gel electrophoresis bared the greatest problems: very often the bands were just too faint to clearly decide whether it is heterozygous for the BRAF V600E mutation or homozygous for the wild type.

For these reasons, the data gained by restriction digest was excluded from this diploma thesis.

Conclusion

According to Colomba et al., Long et al. and Ihle et al., immunohistochemistry is a highly specific and sensitive method (90-100% sensitivity and specificity) for the detection of a BRAF V600E mutation, also when compared to other methods (59, 68, 71). False negatives have rarely been detected in IHC, but false positive are sometimes the case (71, 72). Still, the molecular methods showed a greater sensitivity and specificity and should therefore be the means of choice for testing for the BRAF V600E mutation in clinical settings.

Derived from this experiment, visual evaluation of IHC with Nova Red or Vina Green can be recommended for research settings only or as a pre-testing method in clinical BRAF V600E mutation detection. A refined protocol with the use of an autostainer is suggested though and stringent scoring criteria need to be applied.

Computer-aided evaluation would need to be refined and cannot be recommended at this stage, neither can the restriction digest method be advised to be used.

Thus the null hypothesis can be rejected to some extent, as the BRAF V600E mutation in malignant melanoma could be identified by visual evaluation of IHC with Nova Red or Vina Green in a great number of samples. At this stage molecular methods should be given preference though, especially in clinical applications.

References

1. Garside B. The Growth Factor Receptor and MAPK / ERK Pathway Part 2 2014 [cited 2015 March 11]. Available from: https://www.youtube.com/watch?v=uZdOVp92tjo.
2. Garside B. The Growth Factor Receptor and MAPK / ERK Pathway Part 3 2014 [cited 2015 March 11]. Available from: https://www.youtube.com/watch?v=i65w9xihqEY.
3. Garside B. The Growth Factor Receptor and MAPK / ERK Pathway Part 1 2014 [cited 2015 March 11]. Available from: https://www.youtube.com/watch?v=JAvPB8Om7PI.
4. AperioTechnologies. Aperio Positive Pixel Count Algorithm User's Guide. Vista, CA2009.
5. Erdei E, Torres SM. A new understanding in the epidemiology of melanoma. Expert Rev Anticancer Ther. 2010;10(11):1811-23.
6. Eccles MR. Melanoma genetics/genomics. Front Oncol. 2013;3:309.
7. Whiteman D, Green A. Epidemiology of Malignant Melanoma. In: Dummer R, Pittelkow MR, Iwatsuki K, Green A, Elwan NM, editors. Skin Cancer - A World-Wide Perspective. Berlin, Heidelberg: Springer; 2011. p. 13-26.
8. Garbe C, Peris K, Hauschild A, Saiag P, Middleton M, Spatz A, et al. Diagnosis and treatment of melanoma: European consensus-based interdisciplinary guideline. Eur J Cancer. 2010;46(2):270-83.
9. Liu F, Bessonova L, Taylor TH, Ziogas A, Meyskens FL, Jr., Anton-Culver H. A unique gender difference in early onset melanoma implies that in addition to ultraviolet light exposure other causative factors are important. Pigment Cell Melanoma Res. 2013;26(1):128-35.
10. Crombie IK. Variation of melanoma incidence with latitude in North America and Europe. Br J Cancer. 1979;40(5):774-81.
11. Walker G, Hacker E. Ultraviolet Light as a Modulator for Melanoma Development. In: Murph M, editor. Research on Melanoma - A Glimpse into Current Directions and Future Trends: Intech; 2011. p. 197-228.
12. Autier P, Dore JF. Influence of sun exposures during childhood and during adulthood on melanoma risk. EPIMEL and EORTC Melanoma Cooperative Group. European Organisation for Research and Treatment of Cancer. Int J Cancer. 1998;77(4):533-7.
13. Gershenwald J. Prognostic Factors and Staging in Melanoma. In: Rigel DS, Robinson JK, Ross M, Friedman RJ, Cockerell CJ, Lim HW, et al., editors. Cancer of the Skin. 2 ed: Elsevier Saunders; 2001. p. 282-94.
14. Nagore E, Requena C, Traves V, Guillen C, Hayward NK, Whiteman DC, et al. Prognostic value of BRAF mutations in localized cutaneous melanoma. J Am Acad Dermatol. 2014;70(5):858-62 e1-2.
15. Russak JE, Rigel DS, Friedman RJ. The Importance of Early Detection of Melanoma, Physician and Self-Examination. In: Rigel DS, Robinson JK, Ross M, Friedman RJ, Cockerell CJ, Lim HW, et al., editors. Cancer of the Skin. 2 ed: Elsevier Saunders; 2011. p. 272-80.
16. Ricotti C, Cather J, Cockerell CJ. Pathology of Melanoma: Interpretation and New Concepts. In: Rigel DS, Robinson JK, Ross M, Friedman RJ, Cockerell CJ, Lim HW, et al., editors. Cancer of the Skin. 2 ed: Elsevier Saunders; 2011. p. 295-317.
17. Bataille V. Genetic epidemiology of melanoma. Eur J Cancer. 2003;39(10):1341-7.
18. Ascierto P, Kirkwood J, Grob J-J, Simeone E, Grimaldi A, Maio M, et al. The role of BRAF V600 mutation in melanoma. J Transl Med. 2012;10(1):85.
19. Menzies AM, Lum T, Wilmott JS, Hyman J, Kefford RF, Thompson JF, et al. Intrapatient homogeneity of BRAFV600E expression in melanoma. Am J Surg Pathol. 2014;38(3):377-82.

20. Fisher DE, Kwong LN, Chin L. Molecular Biology of Cutaneous Melanoma. In: DeVita VT, Lawrence TS, Rosenberg SA, editors. Cancer - Principles & Practice of Oncology. 8 ed. Philadelphia: Lippincott Williams & Wilkins; 2008. p. 1889-97.
21. Emuss V, Garnett M, Mason C, Marais R. Mutations of C-RAF are rare in human cancer because C-RAF has a low basal kinase activity compared with B-RAF. Cancer Res. 2005;65(21):9719-26.
22. Alberts B, Bray D, Hopkin K, Johnson A, Lewis J, Raff M, et al. Cell Signaling. In: Morales M, editor. Essential Cell Biology. 4 ed. New York, Abingdon2014. p. 525-63.
23. Sumimoto H, Imabayashi F, Iwata T, Kawakami Y. The BRAF-MAPK signaling pathway is essential for cancer-immune evasion in human melanoma cells. J Exp Med. 2006;203(7):1651-6.
24. Wagener C, Artindustries. Onkoview- Videos zur molekularen Onkologie [Video]. 2009 [cited 2015 Jan 1]. Available from: http://www.onkoview.com/das-buch/signalwege-der-tumorentsstehung/der-map-kinase-mapk--signalweg.html.
25. Hodis E, Watson IR, Kryukov GV, Arold ST, Imielinski M, Theurillat JP, et al. A landscape of driver mutations in melanoma. Cell. 2012;150(2):251-63.
26. Davies H, Bignell GR, Cox C, Stephens P, Edkins S, Clegg S, et al. Mutations of the BRAF gene in human cancer. Nature. 2002;417(6892):949-54.
27. Kamarashev J, LeSchärer L, Zipser MC, Lockwood LL, Dummer R, Krengel S. Melanocytic Tumors. In: Dummer R, Pittelkow MR, Iwatsuki K, Green A, Elwan NM, editors. Skin Cancer - A World-Wide Perspective. Berlin, Heidelberg: Springer; 2011. p. 169-96.
28. Slingluff CL, Flaherty K, Rosenberg SA, Read PW. Cutaneous Melanoma. In: DeVita VT, Lawrence TS, Rosenberg SA, editors. Cancer - Principles & Practice of Oncology. Philadelphia: Lippincott Williams & Wilkins; 2008. p. 1897-951.
29. Balch CM, Gershenwald JE, Soong SJ, Thompson JF, Atkins MB, Byrd DR, et al. Final version of 2009 AJCC melanoma staging and classification. J Clin Oncol. 2009;27(36):6199-206.
30. Fritsch P, Zelger B, Sepp N. Tumoren der Haut. In: Fritsch P, editor. Dermatologie Venerologie. 2 ed: Springer; 2004. p. 585-698.
31. Volkenandt M. Maligne Melanome. In: Braun-Falco O, Plewig G, Wolff H, Burgdorf W, Landthaler M, editors. Dermatologie und Venerologie2005. p. 1313-24.
32. Kolm I, Dummer R, Braun RP. Dermoscopy. In: Dummer R, Pittelkow MR, Iwatsuki K, Green A, Elwan NM, editors. Skin Cancer - A World-Wide Perspective. Berlin, Heidelberg: Springer; 2011. p. 373-8.
33. Knußmann-Hartig E. Dermatologische Diagnostik. In: Moll I, editor. Duale Reihe - Dermatologie. 7 ed. Stuttgart: Thieme; 2010. p. 26-40.
34. Moll I, Jung EG. Benigne Tumoren und Nävi. In: Moll I, editor. Duale Reihe - Dermatologie. 7 ed: Thieme; 2010. p. 287-300.
35. DeVita VT, Lawrence TS, Rosenberg SA. Cancer - Principles & Practice of Oncology. 8 ed. Philadelphia: Lippincott Williams & Wilkins; 2008.
36. Hauswirth U. Maligne Tumoren und Paraneoplasien. In: Moll I, editor. Duale Reihe - Dermatologie. 7 ed. Stuttgart: Thieme; 2010. p. 302-28.
37. Fisher KE, Cohen C, Siddiqui MT, Palma JF, Lipford EH, 3rd, Longshore JW. Accurate detection of BRAF p.V600E mutations in challenging melanoma specimens requires stringent immunohistochemistry scoring criteria or sensitive molecular assays. Hum Pathol. 2014;45(11):2281-93.
38. Deutsche-Dermatologische-Gesellschaft, Arbeitsgemeinschaft-Dermatologische-Onkologie. Malignes Melanom - S3-Leitlinie "Diagnostik, Therapie und Nachsorge des Melanoms". Leitlinienprogramm Onkologie. Berlin2013.

39. Brown MP, Long GV. The use of vemurafenib in Australian patients with unresectable or metastatic melanoma containing the V600 BRAF gene mutation. Asia Pac J Clin Oncol. 2014;10 Suppl S3:1-15.
40. Flaherty KT, Puzanov I, Kim KB, Ribas A, McArthur GA, Sosman JA, et al. Inhibition of mutated, activated BRAF in metastatic melanoma. N Engl J Med. 2010;363(9):809-19.
41. Sosman JA, Kim KB, Schuchter L, Gonzalez R, Pavlick AC, Weber JS, et al. Survival in BRAF V600-mutant advanced melanoma treated with vemurafenib. N Engl J Med. 2012;366(8):707-14.
42. Hersey P. Community experience of vemurafenib for BRAF(V600) melanoma. Lancet Oncol. 2014;15(4):369-70.
43. Larkin J, Del Vecchio M, Ascierto PA, Krajsova I, Schachter J, Neyns B, et al. Vemurafenib in patients with BRAFV600 mutated metastatic melanoma: an open-label, multicentre, safety study. Lancet Oncol. 2014;15(4):436-44.
44. Menzies AM, Long GV, Murali R. Dabrafenib and its potential for the treatment of metastatic melanoma. Drug Des Devel Ther. 2012;6:391-405.
45. Sufficool KE, Hepper DM, Linette GP, Hurst EA, Lu D, Lind AC, et al. Histopathologic characteristics of therapy-associated cutaneous neoplasms with vemurafenib, a selective BRAF kinase inhibitor, used in the treatment of melanoma. J Cutan Pathol. 2014.
46. Sullivan RJ, Flaherty KT. Resistance to BRAF-targeted therapy in melanoma. Eur J Cancer. 2013;49(6):1297-304.
47. Flaherty KT, Infante JR, Daud A, Gonzalez R, Kefford RF, Sosman J, et al. Combined BRAF and MEK inhibition in melanoma with BRAF V600 mutations. N Engl J Med. 2012;367(18):1694-703.
48. Jang S, Atkins MB. Which drug, and when, for patients with BRAF-mutant melanoma? Lancet Oncol. 2013;14(2):e60-9.
49. Arkenau HT, Kefford R, Long GV. Targeting BRAF for patients with melanoma. Br J Cancer. 2011;104(3):392-8.
50. Acharya UH, Jeter JM. Use of ipilimumab in the treatment of melanoma. Clin Pharmacol. 2013;5(Suppl 1):21-7.
51. Homet B, Ribas A. New drug targets in metastatic melanoma. J Pathol. 2014;232(2):134-41.
52. Lang G. Histotechnik - Praxislehrbuch für die Biomedizinische Analytik. 2 ed. Vienna: Springer; 2013.
53. Boenisch T. Antibodies. In: Kumar GL, Rudbeck L, editors. Immunohistochemical Staining Methods - Education Guide. California2009. p. 1-10.
54. Kutzner H, Palmedo G. Immunhistologische Techniken. In: Kerl H, Garbe C, Cerroni L, Wolff H, editors. Histopathologie der Haut. 1 ed. Berlin Heidelberg New York: Springer; 2003. p. 17-41.
55. Routhier CA, Mochel MC, Lynch K, Dias-Santagata D, Louis DN, Hoang MP. Comparison of 2 monoclonal antibodies for immunohistochemical detection of BRAF V600E mutation in malignant melanoma, pulmonary carcinoma, gastrointestinal carcinoma, thyroid carcinoma, and gliomas. Hum Pathol. 2013;44(11):2563-70.
56. Boenisch T. Basic Immunochemistry. In: Kumar GL, Rudbeck L, editors. Immunohistochemical Staining Methods - Education Guide. California2009. p. 11-4.
57. Braun-Falco M, Schempp W, Weyers W. Molecular diagnosis in dermatopathology: what makes sense, and what doesn't. Exp Dermatol. 2009;18(1):12-23.
58. AperioTechnologies. ScanScope XT/XT2 System. Vista, CA2007.
59. Ihle M, Fassunke J, Konig K, Grunewald I, Schlaak M, Kreuzberg N, et al. Comparison of high resolution melting analysis, pyrosequencing, next generation

sequencing and immunohistochemistry to conventional Sanger sequencing for the detection of p.V600E and non-p.V600E BRAF mutations. BMC Cancer. 2014;14(1):13.
60. Macherey-Nagel. DNA isolation from FFPE samples - User manual Nucleo Spin FFPE DNA. Düren2012.
61. Volkenandt M, Degitz K, Sander CA. Molekularbiologische Techniken. In: Kerl H, Garbe C, Cerroni L, Wolff H, editors. Histopathologie der Haut. Berlin Heidelberg New York: Springer; 2003. p. 61-71.
62. Stark M. Designing a Primer for Restriction Digest Method to Test for BRAF V600E Mutation [Laboratory Book]. Brisbane, Australia: QIMR; 2003. p. 46-7.
63. Chang HW, Chuang LY, Cheng YH, Hung YC, Wen CH, Gu DL, et al. Prim-SNPing: a primer designer for cost-effective SNP genotyping. Biotechniques. 2009;46(6):421-31.
64. Roberts RJ, Macelis D. REBASE--restriction enzymes and methylases. Nucleic Acids Res. 2001;29(1):268-9.
65. AgenaBioscience. Oncocarta Panel 2014 [cited 2015 March 11]. Available from: http://agenabio.com/oncocarta-panel.
66. AgenaBioscience. Ultraseek Oncogene Panel 2014 [cited 2015 March 11]. Available from: http://agenabio.com/ultraseek-oncogene-panel.
67. Loes IM, Immervoll H, Angelsen JH, Horn A, Geisler J, Busch C, et al. Performance comparison of three BRAF V600E detection methods in malignant melanoma and colorectal cancer specimens. Tumour Biol. 2015;36(2):1003-13.
68. Colomba E, Helias-Rodzewicz Z, Von Deimling A, Marin C, Terrones N, Pechaud D, et al. Detection of BRAF p.V600E mutations in melanomas: comparison of four methods argues for sequential use of immunohistochemistry and pyrosequencing. J Mol Diagn. 2013;15(1):94-100.
69. Affolter K, Samowitz W, Tripp S, Bronner MP. BRAF V600E mutation detection by immunohistochemistry in colorectal carcinoma. Gene Chromosome Canc. 2013;52(8):748-52.
70. Ilie M, Long E, Hofman V, Dadone B, Marquette CH, Mouroux J, et al. Diagnostic value of immunohistochemistry for the detection of the BRAFV600E mutation in primary lung adenocarcinoma Caucasian patients. Ann Oncol. 2013;24(3):742-8.
71. Long GV, Wilmott JS, Capper D, Preusser M, Zhang YE, Thompson JF, et al. Immunohistochemistry is highly sensitive and specific for the detection of V600E BRAF mutation in melanoma. Am J Surg Pathol. 2013;37(1):61-5.
72. Kuan SF, Navina S, Cressman KL, Pai RK. Immunohistochemical detection of BRAF V600E mutant protein using the VE1 antibody in colorectal carcinoma is highly concordant with molecular testing but requires rigorous antibody optimization. Hum Pathol. 2014;45(3):464-72.
73. Pusch W, Wurmbach JH, Thiele H, Kostrzewa M. MALDI-TOF mass spectrometry-based SNP genotyping. Pharmacogenomics. 2002;3(4):537-48.
74. Stanssens P, Zabeau M, Meersseman G, Remes G, Gansemans Y, Storm N, et al. High-throughput MALDI-TOF discovery of genomic sequence polymorphisms. Genome Res. 2004;14(1):126-33.
75. Liu H, Li Z, Wang Y, Feng Q, Si L, Cui C, et al. Immunohistochemical detection of the BRAF V600E mutation in melanoma patients with monoclonal antibody VE1. Pathol Int. 2014;64(12):601-6.

Appendix

Raw Data:

Sample Number	Visual Evaluation Nova Red	Visual Evaluation Vina Green	PC Positivity Nova Red	PC Positivity Vina Green	BRAF V660E (MelaCarta + Ultraseek)
1	0		0,00036767		0
2	0		0,01335640		1
3	0	0	0,00330417	0,00017863	0
4	0	0	0,01341600	0,00029695	0
5	0		0,07444810		0
6	0		0,00032965		0
7	0	1	0,02777390	0,16835100	0
8	2	2	0,00123009	0,07225680	1
9	2		0,02115560		1
10	0	0	0,00132393	0,00114595	0
11	3		0,10665200		1
12	0	0	0,00325965	0,00037381	0
13	1		0,02345500		0
14	0	0	0,00014307	0,00020659	0
15	0		0,01305780		0
16	3		0,01173830		1
17	0	0	0,09595800	0,00021720	0
18	0		0,00522507		0
19	0		0,00423947		0
20	0	0	0,00132084	0,00000000	0
21	0		0,00298639		0
22	2		0,00622310		0
23	0		0,00068346		0
24	0	0	0,01229750	0,00033825	0
25	3		0,10783900		0
26	1	0	0,00153727	0,00007478	0
27	0		0,00376110		0
28	0	0	0,00959492	0,00018850	0
29	0		0,00016623		0
30	0		0,00097900		0
31	3		0,00343493		1
32	0	0	0,03742630	0,00006805	0
33	1	1	0,11580500	0,02798470	0
34	0	0	0,01927690	0,00010778	0
35	2	0	0,14192700	0,00003993	1
36	1	0	0,01461130	0,00000873	0
37	3		0,11621300		1
38	3	1	0,10520400	0,00239803	1
39	0		0,04995870		0
40	2		0,18382500		1
41	2	0	0,34008800	0,00024745	1
42	0		0,00910568		1
43	1	1	0,00409459	0,00453929	0
44	0	0	0,05171670	0,00134096	0
45	1		0,11873900		1
46	0		0,04464950		0
47	0	0	0,00029953	0,00085343	0

48	0	1	0,00616710	0,00888089	0
49	3	3	0,26095000	0,17118200	1
50	0	1	0,00115296	0,01325800	0
51	0	0	0,00944168	0,00053555	0
52	0		0,00435335		1
53	0		0,00123384		0
54	1	1	0,18024500	0,00019959	1
55	1	1	0,07658950	0,00882828	0
56	1	0	0,38196200	0,00000792	0
57	2		0,00778621		0
58	0	1	0,19258300	0,00205773	0
59	1		0,21964200		0
60	1		0,01296240		1
61	3		0,43271400		1
62	0	0	0,04505400	0,00319645	0

Key for "Visual Evaluation Nova Red" and "Visual Evaluation Vina Green":

0- Negative

1- Questionable positive

2- Weak positive

3- Strong positive

Key for "PC Positivity Nova Red" and "PC Positivity Vina Green"

The figure is multiplied by 100 to obtain the percentage of stained area in the field marked on the slide: "Staining positivity (%)".

Key for and "BRAF V660E (MelaCarta + Ultraseek)":

0- Negative

1- Positive

The data for Restriction Digest is questionable.